



The effect of biological particles and their ageing processes on aerosol radiative properties: Model sensitivity studies

5 Minghui Zhang¹, Amina Khaled¹, Pierre Amato¹, Anne-Marie Delort¹, and Barbara Ervens¹

¹Université Clermont Auvergne, CNRS, SIGMA Clermont, Institut de Chimie de Clermont-Ferrand, 63000
Clermont-Ferrand, France

Corresponding author: Minghui Zhang (minghui.zhang@uca.fr)

10

Abstract. Biological aerosol particles (BAPs) such as bacteria, viruses, fungi and pollen, represent a small fraction of the total aerosol burden. However due to their unique properties, they have been suggested to be important in for radiative forcing by the aerosol direct and indirect effects. By means of process model studies, we compare the sensitivity of these radiative effects to various physicochemical BAP properties (e.g. number concentration, diameter, hygroscopicity, surface tension, contact angle between ice and particles). Exceeding previous sensitivity studies, we explore not only the variability of these properties among different BAP types, but also the extent to which chemical (e.g. nitration), physical (e.g. fragmentation) and biological (e.g. bacteria cell generation) ageing processes of BAPs can modify these properties. Our model results lead to a ranking of the various properties for the radiative effects: (i) Given that BAPs contribute ~0.1% to total cloud condensation nuclei (CCN) number concentration, their effect on total CCN is likely small. (ii) BAPs number fraction of large particles (diameter > ~0.5 μm) is much higher, resulting in a relatively more important effect on direct radiative forcing. (iii) In mixed-phase clouds at $T > -10$ °C, BAPs can contribute ~100% to ice nuclei (IN), which makes their role as IN the most important. Our study highlights the need of implementing ageing processes of different BAPs into models as BAP size, CCN and IN activity and optical properties may be sufficiently altered to affect BAP's residence time and survival in the atmosphere. In particular, we suggest the potential role of biological processes, that are currently not included in aerosol models due to the sparsity of comprehensive data, could affect physicochemical BAP properties.

15
20
25



1 Introduction

30 Biological aerosol particles (BAPs) contribute a small fraction (50 Tg yr⁻¹, with an upper limit of 1000 Tg yr⁻¹) to the total natural global aerosol emissions of ~2900-13000 Tg yr⁻¹ (Stocker et al., 2013). They consist of bacteria, proteins, viruses, fungi, pollen and other biologically-derived materials with potentially infectious, allergenic, or toxic properties (Fröhlich-Nowoisky et al., 2016). They have attracted great interest in the atmospheric science and public health community as they might affect the climate and be responsible
35 for spreading diseases (Asadi et al., 2020; Behzad et al., 2018).

Their mass (Graham et al., 2003; Heald and Spracklen, 2009), number concentrations (Huffman et al., 2013; Matthias-Maser et al., 1999), and fractions (Jaenicke, 2005) can greatly vary depending on the location (Schumacher et al., 2013; Shen et al., 2019; Wei et al., 2016; Yu et al., 2016), time of day (Kang et al., 2012) and other conditions (Graham et al., 2003; Jiaxian et al., 2019; Wu et al., 2016). For example, in the
40 Amazonian rainforest, BAPs contribute ~20% to the mass of submicron organic aerosol (Schneider et al., 2011). In an urban area in Mainz in central Europe, the number fraction was 5-50% for particles with diameter (D) > 0.4 μm (Jaenicke, 2005). Above the ocean, 1% of particles with 0.2 μm < D < 0.7 μm contain biological material (Pósfai et al., 1998). Temporal variability of BAPs was observed exhibiting peaks in the morning, during and after rain (Huffman et al., 2013; Zhang et al., 2019). To the total global BAP emissions,
45 bacteria contribute 0.4-1.8 Tg yr⁻¹, which is less than 25-31 Tg yr⁻¹ by fungal spores (Heald and Spracklen, 2009; Hoose et al., 2010) and 47 Tg yr⁻¹ by pollen (Burrows et al., 2009a, 2009b). Although the mass fraction of bacteria is small, their number concentration (~0.001-1 cm⁻³) (Lighthart and Shaffer, 1995; Tong and Lighthart, 2000) is larger than that of fungal spores (~0.001-0.01 cm⁻³) and pollen (~0.001 cm⁻³) (Huffman et al., 2010). The concentration of viruses can reach up to ~0.1 cm⁻³ in indoor air (Prussin et al., 2015) and
50 decreases to ~0.01 cm⁻³ outdoors (Després et al., 2012; Weesendorp et al., 2008). The comparably small size of viruses and bacteria (D_{viruses} ~0.1 μm, D_{bacteria} ~1 μm, D_{pollen} ~10 μm) enables relatively long residence times of several days in the atmosphere (Burrows et al., 2009a; Verreault et al., 2008).

In numerous recent review articles, it has been suggested that BAPs can affect radiative forcing in multiple ways (**Figure 1**) (Coluzza et al., 2017; Després et al., 2012; Haddrell and Thomas, 2017; Hu et al., 2018;
55 Šantl-Temkiv et al., 2020; Smets et al., 2016): BAPs might directly interact with radiation by scattering or absorbing light (**Figure 1a**). While their aerosol direct effect is likely globally small due to low BAP number concentration (Löndahl et al., 2014), it may be of greater interest locally and for specific wavelength ranges due to the large size of BAPs (Myhre et al., 2013). The optical properties of BAPs (Arakawa et al., 2003; Hu et al., 2019; Thrush et al., 2010) resemble those of other organic particles as BAPs are largely composed
60 of proteins and other macromolecules. Accordingly, BAPs' optical properties can be ascribed to specific organic functional entities such as amino groups or aromatic structures (Hill et al., 2015; Hu et al., 2019).



At subsaturated relative humidity (RH) conditions, the hygroscopicity (κ_{BAP}) determines their ability to take up water (Petters and Kreidenweis, 2007) and thus their equilibrium size, which affects their direct radiative properties. Their hygroscopicity shows a large range ($0.03 \leq \kappa_{\text{BAP}} \leq 0.25$), which is explained by variation of surface composition due to different types of BAPs and/or ageing processes (Bauer et al., 2003; Haddrell and Thomas, 2017; Šantl-Temkiv et al., 2020; Sun and Ariya, 2006).

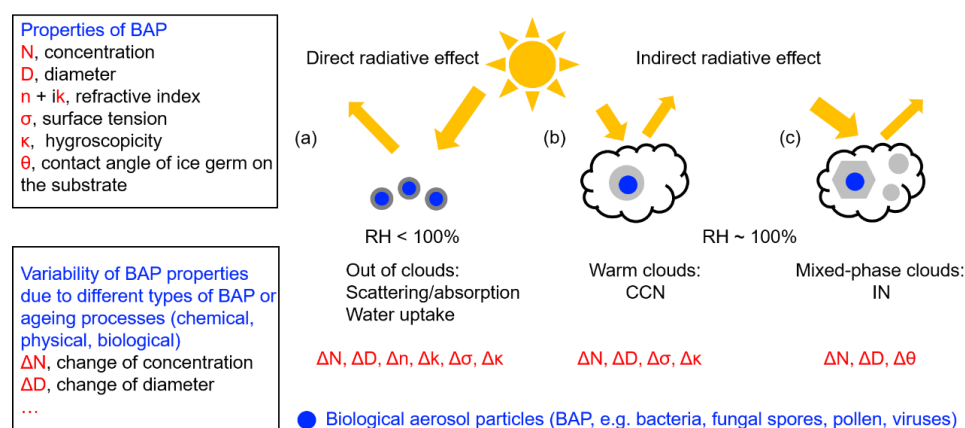


Figure 1. Schematic of the influence of BAP properties and ageing processes on direct and indirect radiative effects. (a) The direct radiative forcing is influenced by BAP concentration (N_{BAP}), diameter (D_{BAP}), refractive index ($m_{\text{BAP}} = n + ik$), surface tension (σ_{BAP}), and hygroscopicity (κ_{BAP}) affect scattering/absorption of aerosol populations at $RH < 100\%$. (b) N_{BAP} , D_{BAP} , surface tension of aqueous particles (σ_{BAP}), and hygroscopicity (κ_{BAP}) affect CCN activity and properties of warm clouds. (c) N_{BAP} , D_{BAP} , and contact angle of ice germ on the substrate (θ_{BAP}) affect the evolution of mixed-phase clouds.

Convective and precipitating clouds lead to efficient particle redistribution by vertical transport and removal of particles by wet deposition. Therefore, cloud-related physicochemical properties need to be constrained to determine the distribution and residence time of BAPs in the atmosphere. Since BAPs often have supermicron sizes, they may act as ‘giant CCN’ and thus induce early precipitation (Barahona et al., 2010; DeLeon-Rodriguez et al., 2013; Feingold et al., 1999). Based on a global model study of BAPs, it was concluded that CCN-relevant properties need to be refined in order to further probe their role in the climate system (Konstantinidis, 2014). Several experimental studies have explored the CCN properties of BAPs and determined their hygroscopicity (κ) (Ariya et al., 2009; Sun and Ariya, 2006). The role of biosurfactant production by bacteria and fungi has been also discussed in the context of their CCN activity since a lower surface tension (σ_{BAP}) enhances water uptake (Renard et al., 2016). In addition, biosurfactant molecules that are produced by bacteria and fungi, while they reside on leaves or other surfaces, might attach to other particles, thus, increasing their CCN ability as well.



In addition to acting as CCN, some species of plant pathogen bacteria and fungi can nucleate ice at $T > -10^{\circ}\text{C}$ (Hoose and Möhler, 2012; Morris et al., 2004, 2008; Pouzet et al., 2017), which makes them unique in terms of ice nucleation to affect the evolution of mixed-phase clouds at these temperatures (**Figure 1c**). Above vegetated forests (Tobo et al., 2013) and near the surface of the Southern Ocean (Burrows et al., 2013), BAPs have been shown to contribute significantly to the total abundance of IN: In a high altitude mountain region of the United States, ambient measurements suggest that 16-76% of IN at -30°C consist of primary biological material (Pratt et al., 2009); a similar proportion (33%) was reported at -31 to -34°C in the Amazon basin (Prenni et al., 2009).

The radiative impacts of BAPs, influenced by the physicochemical properties (N_{BAP} , D_{BAP} , κ_{BAP} , σ_{BAP} , m_{BAP} , θ_{BAP}), summarized in **Figure 1**, can largely differ on spatial and temporal scales, leading to different conclusions regarding the climatic impacts of BAPs (Burrows et al., 2009a, 2009b; Hoose et al., 2010; Junge and Swanson, 2008; Konstantinidis, 2014; Sahyoun et al., 2017; Sesartic et al., 2012). These properties are even more variable than represented in current models as BAPs undergo chemical, physical and biological ageing processes (Coluzza et al., 2017; Deguillaume et al., 2008; Pöschl, 2005; Vaïtilingom et al., 2010).

- *Physical* transformations include agglomeration/fragmentation of cells (Coluzza et al., 2017; Lighthart, 1997; Zhang et al., 2019), coating with organic or inorganic components (Pöschl and Shiraiwa, 2015; Joly et al., 2015), or with solid ice or liquid water (Joly et al., 2013). These processes might alter various physicochemical properties listed in **Figure 1**.
- *Chemical* transformations include oxidation (Jayaraman et al., 2008; Vaïtilingom et al., 2010), nitration (Franze et al., 2005), oligomerization (Tolocka et al., 2004), degradation of macromolecules (Estillore et al., 2016), and changes of the protein conformations due to exposure to different pH values (Kristinsson and Hultin, 2004). These reactions lead to the modification of the protein structures and other macromolecules and thus affect BAP optical properties (Myhre et al., 2013), CCN activity (Sun and Ariya, 2006), and IN ability (Attard et al., 2012; Kunert et al., 2019).
- *Biological* processes might be initiated by living microorganisms in BAPs, unlike in other aerosol particles in the atmosphere (Amato et al., 2017; Delort et al., 2017; Joly et al., 2015). Such processes are generally driven by strategies to adapt to the harsh conditions in the atmosphere (e.g., rapid temperature and RH changes, thaw/freezing cycles, humidification/desiccation, UV exposure) (Hamilton and Lenton, 1998; Horneck et al., 1994; Joly et al., 2015; Setlow, 2007) or to limit their atmospheric residence time by initiating precipitation (Hernandez and Lindow, 2019). These processes include nutrient uptake by biodegradation (Khaled et al., 2020), bacteria cell generation that enhances particle size and surface area (Ervens and Amato, 2020), formation of biofilms (extracellular polymeric substances) which enables BAPs to form aggregates (Monier and Lindow, 2003, 2005; Morris et al., 2008; Sheng et al., 2010),



120 expression of ice-nucleating proteins (Joly et al., 2013; Kjelleberg and Hermansson, 1984), formation of
biosurfactants that enhances water uptake (Hernandez and Lindow, 2019; Neu, 1996), desiccation that
decreases size of BAPs (Barnard et al., 2013), formation of pigments (Pšenčík et al., 2004; Fong et al.,
2001) enhancing light absorption, fungal spore germination (Ayerst, 1969) or formation of bacteria
endospores (Enguita et al., 2003) that increases the N_{BAP} , and metabolism of cellular components
(membranes, proteins, saccharides, osmolytes, etc) (Fox and Howlett, 2008; Xie et al., 2010). To date,
125 the uncertainties introduced by these BAP ageing processes in the estimate of BAP radiative effects, their
atmospheric residence time and distribution can only be assessed qualitatively due to the lack of
comprehensive data. However, it may be expected that some of them lead to similar differences in BAP
properties than differences between BAP types.

In our study, we give a brief overview of the BAP properties in *Figure 1* and summarize which *chemical*,
130 *physical* and *biological* processes may alter these properties (*Section 2*). By means of process models
(*Section 3*), we explore in a simplistic way the relative importance of these BAP properties and ageing
processes for their radiative effects depicted in *Figure 1* (*Section 4*). The results of our sensitivity studies
allow a ranking of the importance of the various BAP properties and processes in terms of their radiative
impacts. In *Section 5*, we give some guidance on the need of future laboratory, field and model studies to
135 more accurately describe the radiative effects, distribution and residence time of BAPs in the atmosphere.

2. Physicochemical properties and processes of BAPs

Literature data on physicochemical parameters of BAPs are summarized in *Table 1*. It is not our goal to
repeat exhaustive reviews on these individual properties; for this, we refer to previous overview articles
(Bauer et al., 2003; Coluzza et al., 2017; Deguillaume et al., 2008; Després et al., 2012; Fröhlich-Nowoisky
140 et al., 2016; Hoose and Möhler, 2012; Huffman et al., 2020; Šantl-Temkiv et al., 2020). We rather aim at
using characteristic orders of magnitude of these properties as input data to our process models (*Section 3*).
Therefore, we only give a brief overview on the ranges and variability of these properties for different BAP
types and due to various ageing processes.

2.1 BAP number size distribution parameters (N_{BAP} and D_{BAP})

145 The number concentration (N_{BAP}) of most BAP types is in the range of $0.001 \leq N_{\text{BAP}} \leq 0.1 \text{ cm}^{-3}$ (*Table 1*).
The number concentration of bacteria is higher than that of fungal spores and pollen although the mass
concentration of bacteria is lower (Burrows et al., 2009a; Heald and Spracklen, 2009; Hoose et al., 2010).
 N_{BAP} can vary by about three orders of magnitude among different ecosystems, locations, seasons, and time
of the day (Huffman et al., 2010, 2020; Matthias-Maser et al., 2000a, 2000b; Schumacher et al., 2013). The
150 BAP diameter (D_{BAP}) covers a broad range of $0.01 \mu\text{m} \leq D_{\text{BAP}} \leq 100 \mu\text{m}$. This parameter usually refers to
the mass equivalent diameter, which is the diameter of a sphere with the same mass as a non-spherical



BAP. The size depends on the types of BAPs, and on changes due to biological and physical processing. Viruses are reported to be the smallest BAP types ($0.01 \mu\text{m} \leq D_{\text{viruses}} \leq 0.3 \mu\text{m}$) while pollen is the largest ($5 \mu\text{m} \leq D_{\text{pollen}} \leq 100 \mu\text{m}$) (**Table 1**). Biological processing, such as cell generation, might increase the size of particles by producing secondary biological aerosol mass (Ervens and Amato, 2020; Sattler et al., 2001). Typical bacterial cell generation rates are in the range of $0.1\text{--}0.9 \text{ h}^{-1}$ (Ervens and Amato, 2020). Efficient generation in the atmosphere is assumed to be largely restricted to the time of cell exposure to liquid water (i.e., in-cloud). With an average atmospheric residence time of ~ 1 week (Burrows et al., 2009b) and an average in-cloud time fraction of $\sim 15\%$ (Lelieveld and Crutzen, 1990), it can be estimated that the generation time scale of bacteria cells in the atmosphere is on the order of ~ 20 h. Thus, for example, D_{bacteria} may increase from $1 \mu\text{m}$ to $2 \mu\text{m}$ after one week in the atmosphere assuming a generation rate of 0.3 h^{-1} . Other rates, such as the cell growth, are usually much smaller (Marr, 1991; Middelboe, 2000; Price and Sowers, 2004; Sattler et al., 2001; Vrede et al., 2002), and thus, contribute less efficiently to a change in D_{BAP} . In addition, the formation of extracellular polymeric substances might lead to the formation of biofilms, which increase BAP size by forming agglomerate (Monier and Lindow, 2003, 2005). Agglomerate formation might be also described as a physical process, when BAPs (e.g. bacteria) attach to other particles (e.g. dust) (Després et al., 2012; Lighthart, 1997), which can result in particle sizes on the order of $\sim 10 \mu\text{m}$. Similarly, a biologically-driven physical processes might lead to enhancement of N_{BAP} as it has been observed that pollen ruptures into fragments with diameter of $1\text{--}4 \mu\text{m}$ during thunderstorms (Zhang et al., 2019).

2.2 Optical properties of BAPs: Complex refractive index ($m_{\text{BAP}} = n + ik$)

The scattering and absorption of particles are commonly described by the refractive index m_{BAP} with real part (n_{BAP}) and imaginary parts (k_{BAP}) that depend on the chemical composition and wavelength of irradiation. Arakawa et al. (2003) reported $1.5 \leq n_{\text{BAP}} \leq 1.56$ and $3 \cdot 10^{-5} \leq k_{\text{BAP}} \leq 6 \cdot 10^{-4}$ for bacteria (*Erwinia herbicola*) in the wavelength range of $0.3\text{--}2.5 \mu\text{m}$. Other groups found a broader range of n and k (**Table 1**) for different types of BAPs and irradiation wavelengths (Hu et al., 2019; Thrush et al., 2010). The imaginary part can vary by three orders of magnitude for different BAP types (Hu et al., 2019). Hill et al. (2015) showed that the refractive index of BAPs can be estimated based on the chemical composition. They reported $1.59 + i0.045$ for *Bacillus vegetative* cells at $0.266 \mu\text{m}$. Also BAP shape (e.g. core-shell structure, hexagonal grids, and barbs), as it has been demonstrated for pollen, influences the optical properties (Liu and Yin, 2016). Due to the similarity of the molecular structure of organic macromolecules (e.g. proteins) and secondary organic aerosols (SOA), it can be likely assumed that might alter the BAP refractive index similar to that of SOA. Experimental results show $1.516 \leq n \leq 1.576$ and $0 \leq k \leq 0.013$ for fresh SOA; after nitration, the real part changed to $1.534 \leq n \leq 1.594$ and the imaginary part increased to $0.001 \leq k \leq 0.035$ (Liu et al., 2015; Moise et al., 2015).



185 **Table 1.** Physicochemical properties of various types of BAP and their changes due to physical, chemical and biological ageing processes based on literature data.

BAP Types	Physicochemical properties						
	Concentration N_{BAP} (cm^{-3})	Diameter D_{BAP} (μm)	Hygroscopicity κ	Complex refractive index $m_{BAP}(\lambda) = n + ik$	Surface tension σ ($mN m^{-1}$)	IN active number fraction	Contact angle θ_{BAP} ($^{\circ}$)
Bacteria	0.001-1 (1) 0.01-1.4 (2)	1 (7) 0.6-7 (8)	0.11-0.25 (11)	n: 1.5-1.56, k: $3 \cdot 10^{-5}$ - $6 \cdot 10^{-4}$ (17). n: 1.5-1.56, k: 0-0.04 (18). n: 1.25-1.87, k: 0-0.45 (19)	25, 30, 55, 72 (20)	~0.1%, ~1%, ~10% (21)	32-34 (24). 4-20 (25). 28, 33, 44 (26)
Fungal spores	0.001-0.01 (3)	3-5 (4); 1-30 (5)					30-33 (27)
Fern spores	10^{-5} (4)	1-30 (4)					
Pollen	0.001 (5)	5-100 (9)	0.03-0.073 (12). 0.036-0.048 (13). 0.05-0.1 (14). 0.08-0.17 (15). 0.14-0.24 (16)			~100% (22, 23)	14-30 (25). 15, 16.3 (28)
Pollen fragments	0.1 (6)	1-4 (6)					
Viruses	0.01 (4)	0.01-0.3 (4) 0.04-0.2 (10)					
Ageing processes of BAP							
	Physical ageing	Chemical ageing		Biological ageing			
Bacteria	Agglomeration: $\Delta D_{BAP} > 0$, $\Delta N_{BAP} < 0$ (8)	Nitration: $\Delta n_{BAP} \sim 0.02$, $\Delta k_{BAP} \sim 0.03$ (29). Nitration: $\Delta \theta_{BAP} \sim 1^{\circ}$ (26). pH changes: $\Delta \theta_{BAP} \sim 1.5^{\circ}$ (26).		Biosurfactant production: $\sigma_{BAP} < 0$ (20). Biofilm formation: $\Delta D_{BAP} > 0$ (30). Endospore formation: $\Delta N_{BAP} > 0$ (31). Cell generation: $\Delta D_{BAP} > 0$ (32). Desiccation: $\Delta D_{BAP} < 0$ (33). Pigment formation (34, 35): $\Delta k > 0$.			
Fungi				Biosurfactant production: $\sigma_{BAP} < 0$ (20). Germination: $\Delta N_{BAP} > 0$ (34). Desiccation: $\Delta D_{BAP} < 0$ (33).			
Pollen	Rupture: $\Delta D_{BAP} < 0$, $\Delta N_{BAP} > 0$ (6)	Oxidation: $0.5 \leq \Delta \theta_{BAP} \leq 0.8^{\circ}$ (28)					

(1) Total bacteria, Tong and Lighthart et al., 1999; (2) Under haze conditions in Beijing, Wei et al., 2016. (3) Elbert et al., 2007; (4) Després et al., 2012; (5) blooming times, Huffman et al. 2010; (6) thunderstorm times, Zhang et al., 2019; (7) Burrows et al., 2009a; (8) Lighthart 1997; (9) Pöhlker et al., 2013; (10) Verreault et al., 2008; (11) Lee et al., 2002; (12) Pope et al. 2010; (13) Tang et al., 2019; (14) Chen et al., 2019; (15) Griffiths et al., 2012; (16) pollen kit, Prisle et al., 2019; (17) Arakawa et al., 2003; (18) Thrush et al., 2010; (19) Hu et al. 2019; (20) Renard et al., 2016; (21) T $\sim -10^{\circ}C$, immersion freezing, *Pseudomonas syringae* bacteria, *Pseudoxanthomonas* sp., *Xanthomonas* sp., Joly et al., 2013; (22) deposition freezing for pollen, Diehl et al., 2001; (23) immersion and contact freezing for pollen, Diehl et al., 2002; (24) Hoose and Möhler, 2012; (25) Chen et al., 2008; (26) immersion freezing for *Pseudomonas syringae*, and *Pseudomonas fluorescens*, Attard et al., 2012; (27) immersion freezing for fungi, Kunert et al., 2019; (28) deposition freezing of silver birch and grey alder pollen, Gute and Abbatt, 2018; (29) nitrated SOA to represent nitrated BAP, Liu et al., 2015; (30) Morris et al., 2008; (31) Enguita et al., 2003; (32) Ervens and Amato, 2020; (33) Barnard et al., 2013; (34) Pšenčík et al., 2004; (35) Fong et al., 2001.



2.3 BAP Properties relevant for CCN activation

2.3.1 Hygroscopicity (κ_{BAP}) of BAPs

200 The hygroscopicity determines BAP's hygroscopic growth factor (gf, as the ratio of wet to dry particle diameter) at subsaturated conditions and their CCN activity; it is usually expressed as the hygroscopicity parameter κ (Petters and Kreidenweis, 2007). Lee et al. (2002) reported $gf = 1.16$ for *Bacillus subtilis* bacteria and $gf = 1.34$ for *Escherichia coli* bacteria at RH ~85%. Based on these growth factors, $\kappa_{\text{bacteria}} = 0.11$ and $\kappa_{\text{bacteria}} = 0.25$ for these bacteria can be calculated. The hygroscopicity of pollen is similar: The κ value of intact pollen grains falls into the range of $0.03 \leq \kappa_{\text{pollen}} \leq 0.17$ (Chen et al., 2019; Pope, 2010; Tang et al., 2019), in agreement with κ of pollen kitts on the surface of pollen ($0.14 \leq \kappa_{\text{pollen}} \leq 0.24$) (Prisle et al., 2019).

2.3.2 Surface tension (σ_{BAP}) of BAPs

In most model studies that explore CCN activation, it is assumed that particles have a surface tension close to that of water ($\sigma_{\text{water}} = 72 \text{ mN m}^{-1}$). This assumption is likely justified under many conditions due to the strong dilution of internally mixed aerosol particles near droplet activation. There are numerous studies that postulate that surfactants in aerosol particles might influence the surface tension sufficiently to significantly change their CCN activity (Bzdek et al., 2020; Facchini et al., 1999; Lowe et al., 2019; Nozière et al., 2014). These surfactants are usually assumed to have natural sources such as the ocean surface (Gérard et al., 2019; Ovadnevaite et al., 2017). Another source of surfactants might be living microorganisms that produce biosurfactants which enhance surface hygroscopicity and decrease surface tension (Akbari et al., 2018). These biosurfactants might not only be associated with BAP themselves as they might be deposited on surfaces (e.g. leaves) where they can be taken up by other particles. Renard et al. (2016) reported that 41% of tested strains actively produced surfactant with $\sigma_{\text{BAP}} < 55 \text{ mN m}^{-1}$ and 7% of tested strains can produce extremely efficient biosurfactants with $\sigma_{\text{BAP}} < 30 \text{ mN m}^{-1}$. All of these tested strains were collected and isolated in cloud water samples. The efficient biosurfactants ($\sigma_{\text{BAP}} < 45 \text{ mN m}^{-1}$) are mostly produced by *Pseudomonas* and *Xanthomonas* of bacteria (78%) and *Udeniomyces* fungi (11%). For the most efficient biosurfactants, we fit the following linear approximation based on their experiments:

$$\sigma_{\text{BAP}} = 89.6 - 2.9 \cdot C_{\text{biosurf}} \quad \text{if } 6 \text{ mg L}^{-1} \leq C_{\text{biosurf}} \leq 22 \text{ mg L}^{-1} \quad (1)$$

225 where σ_{BAP} is BAP surface tension in (mN m^{-1}) and C_{biosurf} is the biosurfactant concentration in (mg L^{-1}). Higher and lower biosurfactant concentrations may be approximated with 25 mN m^{-1} and 72 mN m^{-1} for simplicity. **Equation 1** implies that the concentration of biosurfactant on the surface is the same as in the bulk. Recent studies suggest that the surface concentration of surfactants is higher than the bulk concentration (Bzdek et al., 2020; Lowe et al., 2019; Ruehl et al., 2016). Thus, a smaller amount of



230 biosurfactants ('critical micelle concentration') than suggested by *Equation 1* might be sufficient to
significantly decrease σ_{BAP} . The biosurfactant concentration depends both on the dilution (amount of water)
and on the mass fraction of biosurfactants in the particle. The mass fraction has not been determined for
biosurfactants; however, other surfactants have been shown to contribute ~0.1% to the total particle mass
(Gérard et al., 2019).

235 **2.4 BAP Properties relevant for ice nucleation**

2.4.1 IN active particle number fraction

In freezing experiments of pollen, it has been demonstrated that all particles freeze at sufficiently low
temperatures, i.e. the IN active number fraction can be assumed as ~100%. Both condensation and
immersion/contact freezing led to frozen fractions of 100% at $T \sim -18^\circ\text{C}$ (Diehl et al., 2001) and $T \sim -20^\circ\text{C}$
240 (Diehl et al., 2002), respectively. However, for bacteria such as *Pseudomonas syringae*, the maximum frozen
fraction only reaches values of 0.1-10% at $T \sim -10^\circ\text{C}$ (Joly et al., 2013). This might be explained by the fact
that not all of the bacteria cells express the same proteins even if they belong to the same species and the
same population. It was observed that bacteria express more IN proteins under stress conditions (Kjelleberg
and Hermansson, 1984), as a strategy to reach nutrients after destroying the cells of plants by freezing.
245 However, to date it is not fully understood why in lab experiments some of the bacteria cells show freezing
behaviour while others from the same population do not and why individual cells show stochastic behaviour
in repeated experiments (Lukas et al., 2020).

2.4.2 Contact angle between substrate and ice (θ_{BAP})

In agreement with previous studies, we base our discussion on the contact angle as a fit parameter in the
250 classical nucleation theory (CNT) to parametrize the frozen fraction observed in experiments. Chen et al.
(2008) reported $4^\circ \leq \theta_{\text{bacteria}} \leq 20^\circ$ and $14^\circ \leq \theta_{\text{pollen}} \leq 30^\circ$. Similarly, based on the measurements by Attard
et al. (2012), we derived values of 28° , 33° , and 44° for different types of bacteria. θ values for fungi based
on the measurements by Kunert et al. (2019) are similar ($30^\circ \leq \theta_{\text{fungi}} \leq 33^\circ$). Gute and Abbatt (2018)
performed deposition freezing experiments of pollen; based on their experiments, we fitted $\theta_{\text{pollen}} = 15^\circ$ for
255 silver birch and $\theta_{\text{pollen}} = 16.3^\circ$ for grey alder. Hoose and Möhler (2012) reported the ice nucleation active
surface site (INAS) density of various bacteria at -5°C ($10^{2.5}$ - 10^{10} m^{-2}). INAS implies that freezing occurs
deterministically as opposed to stochastic freezing described by CNT. As the sensitivity of ice nucleation to
time is generally small compared to other parameters (Ervens and Feingold, 2013), we fitted their data using
CNT and obtained a range of $32^\circ \leq \theta_{\text{bacteria}} \leq 34^\circ$, consistent with other bacteria (Attard et al., 2012).

260 Chemical processes (e.g. nitration) can change the molecular surface of BAPs by e.g., adding nitro groups
to tyrosine residues of proteins (Estillore et al., 2016), which can alter the IN activity. Attard et al. (2012)



measured the cumulative fraction of IN among a population of bacteria before and after nitration for 16–18 h. The residence time of aerosol particles in the atmosphere is from hours to weeks, which means that the experimental nitration times might be a realistic time scale. Based on these data, we calculated that the contact angle increased by $\sim 1^\circ$ after nitration for some bacteria. In contrast, Kunert et al. (2019) reported that protein nitration does not influence the cumulative fraction of IN for 65 species of fungi investigated. In order to study the oxidation effect, Gute and Abbatt (2018) exposed pollen to OH radicals and measured the cumulative frozen fraction of pollen in terms of deposition freezing. We calculated that the contact angle increased by $\sim 0.5^\circ \leq \Delta\theta_{\text{pollen}} \leq 0.8^\circ$ after oxidation. While experimental conditions are often such that a large fraction of particles is nitrated or oxidized, respectively, only a small fraction of ambient proteins ($\sim 0.1\%$) have been found to be only nitrated (Franze et al., 2005). Attard et al., (2012) showed that a decrease of pH from 7.0 to 4.1, led to a decrease of the cumulative fraction of IN of *P. syringae* (32b-74) from 10^{-2} to 10^{-8} at -4°C . This change can be described by an increase of θ from 28.7° to 30.3° ($\Delta\theta_{\text{bacteria}} \sim 1.6^\circ$). *P. syringae* (CC0242), Snomax[®], and *P. fluorescens* exhibited similar increases of $\Delta\theta_{\text{bacteria}} \sim 1.5^\circ$ for the same change in pH.

3. Model description

3.1 Box model: Scattering/absorption of wet particles at RH < 100% calculated by Mie theory

A box model was used to simulate total scattering/absorption based on Mie theory (Bohren, 1983) for a constant aerosol distribution at different RH. Water uptake by particles is calculated based on Köhler theory. Mie theory is applied to calculate total scattering and absorption of the wet aerosol population as a function of D , N , and m at different wavelengths (λ). The input aerosol size distribution is based on ambient measurements by an ultraviolet aerodynamic particle sizer (UV-APS) in central Europe (Zhang et al., 2019) that cannot detect particles with $D < 0.5 \mu\text{m}$. At $\lambda \geq 300 \text{ nm}$, the particles with $D > 3 \mu\text{m}$ interact with light by geometric scattering, rather than Mie scattering. Therefore, we intentionally only consider particles with diameters of $0.5 \mu\text{m} < D < 2.8 \mu\text{m}$ in 24 size classes to represent ambient aerosol particles relevant for our study with a concentration of $N_{\text{other}} = 1.4 \text{ cm}^{-3}$. We consider one additional BAP size class which has specific parameters (N_{BAP} , D_{BAP} , m_{BAP} , κ_{BAP} , σ_{BAP}) that are varied in the sensitivity studies.

Calculations are performed for RH of 10% and 90%, i.e. for different BAP growth factors. In a series of sensitivity studies ($S_{\text{opt1}} - S_{\text{opt11}}$; **Table 2**), we explore the sensitivity of scattering and absorption to the N_{BAP} , D_{BAP} , κ_{BAP} , and m_{BAP} ($m_{\text{BAP}} = n + ik$). We not only compare model results for properties representing different BAP types (e.g. D_{bacteria} vs D_{fungal}), but also explore the ranges of property variation due to ageing processes of individual BAP types (e.g. $\Delta D_{\text{bacteria}}$).



295

Table 2. Model sensitivity studies assume different physicochemical BAP parameters to investigate their effect on the optical properties (*Section 3.1*), CCN activation (*Section 3.2*) and ice nucleation (*Section 3.3*).

Scattering/Absorption:					
0.5 μm < D_{other} < 2.8 μm ; $N_{\text{other}} = 1.4 \text{ cm}^{-3}$; $\kappa_{\text{other}}: 0.3$. $\sigma_{\text{BAP}} = \sigma_{\text{other}} = 72 \text{ mN m}^{-1}$					
Composition of other particles: 90% ammonium sulfate + 10% soot					
Simulation	$N_{\text{BAP}} (\text{cm}^{-3})$	$D_{\text{BAP}} (\mu\text{m})$	$n(\lambda)_{\text{BAP}}; k(\lambda)_{\text{BAP}}$	RH	κ_{BAP}
S_{opt1}	0	-	-	10%	-
S_{opt2}	0.01	1	1.5-1.56; $3 \cdot 10^{-5}$ - $6 \cdot 10^{-4}$		0.25
S_{opt3}	0.1				
S_{opt4}	1				
S_{opt5}	0.1	2			
S_{opt6}		3			
S_{opt7}	1	2			0.03
S_{opt8}					0.25
S_{opt9}				90%	0.03
S_{opt10}					0.25
S_{opt11}			1.25-1.6; 0.001-0.1	10%	
S_{opt12}			1.5-1.85; 0.08-0.5		
S_{opt13}			1.25-1.75; 0.06-0.32		
S_{opt14}			1.3-1.7; 0.05-0.1		
S_{opt15}			1.516-1.576; 0-0.013		
S_{opt16}			1.534-1.594; 0.001-0.035		
Cloud condensation nuclei (CCN):					
5 nm < D_{other} < 7.7 μm ; $N_{\text{other}} = 902 \text{ cm}^{-3}$					
	$D_{\text{BAP}} (\mu\text{m})$	Hygroscopicity κ_{BAP}		Surface tension $\sigma_{\text{BAP}} (\text{mN m}^{-1})$	
S_{CCN1}	0.5	0.25		72	
S_{CCN2}		0.03			
S_{CCN3}	0.1	0.25			
S_{CCN4}		0.03			
S_{CCN5}	0.05	0.25			
S_{CCN6}		0.03			
S_{CCN7}	0.5	0.03		25	
S_{CCN8}	0.1				
S_{CCN9}	0.05				
Ice nuclei (IN):					
46nm < D_{other} < 2.5 μm ; $N_{\text{other}} = 100 \text{ cm}^{-3}$					
$N_{\text{BAP, IN}} / N_{\text{BAP}}: 10\%$					
$\theta_{\text{other}}: 80^\circ$					
	$N_{\text{BAP}} (\text{cm}^{-3})$	$D_{\text{BAP}} (\mu\text{m})$	Contact angle (θ_{BAP}) of ice germ	Cloud temperature ($^\circ\text{C}$)	base
S_{IN1}	1	1	37°	-8	
S_{IN2}	0.01				
S_{IN3}	0.001				
S_{IN4}	0.01	2			
S_{IN5}		5			
S_{IN6}		1	4°	-5.5	
S_{IN7}			20°		
S_{IN8}			40°		
S_{IN9}			38°	-8	



3.2 Adiabatic parcel model

3.2.1 CCN activation in warm clouds

An adiabatic parcel model was applied to simulate the formation of warm clouds (Ervens et al., 2005; Feingold and Heymsfield, 1992). The activation of an aerosol population to cloud droplets is described as a function of N , D , κ , and σ . The dry aerosol size distribution covers a size range of $5 \text{ nm} < D_{\text{other}} < 7.7 \text{ }\mu\text{m}$ with $N_{\text{other}} = 902 \text{ cm}^{-3}$. Similar to the studies on optical properties (*Section 3.1*), we assume that one aerosol size class is composed of biological material for which we vary D_{BAP} , κ_{BAP} , and σ_{BAP} to explore the role of differences in BAP type and ageing processes on cloud droplet activation ($S_{\text{CCN1}} - S_{\text{CCN9}}$, *Table 2*).

3.2.2 Ice nucleation in mixed-phase clouds

The adiabatic parcel model as used for the CCN calculations was extended by the description of immersion freezing based on classical nucleation theory (Ervens et al., 2011). At each model time step (1 second), the frozen fraction of BAP is calculated; if 1% or more of the IN size class are predicted to freeze in a given time step, a new size class of ice particles is generated in the model, for which ice growth is described. We consider an aerosol size distribution with $46 \text{ nm} < D_{\text{other}} < 2.48 \text{ }\mu\text{m}$ in nine size classes and $N_{\text{other}} = 100 \text{ cm}^{-3}$ and one additional BAP size class, which is the only one that includes potentially freezing IN under the model conditions. Similar to the analysis by Ervens et al. (2011), we compare the evolution of the ice liquid water contents (IWC and LWC) expressed in mass fractions [%] whereas 100% corresponds to the total water (ice + liquid + vapor) mixing ratio that is constant under the adiabatic model conditions. Input values of D_{BAP} , N_{BAP} , and θ_{BAP} are varied in simulation $S_{\text{IN1}} - S_{\text{IN9}}$ (*Table 2*).

4. Results and discussion

4.1 Sensitivity of optical properties at subsaturated conditions (RH < 100%) to BAP properties

4.1.1 Influence of concentration (NBAP) and diameter (DBAP) on scattering and absorption

As explained in *Section 3.1*, in the sensitivity studies of optical properties, we consider only particles with D in the same range as λ so that scattering and absorption can be calculated by Mie theory. As ambient aerosol particles also include smaller and larger particles, our conclusions on BAP direct radiative effects should be regarded as the upper limit on total scattering and absorption.

In *Figure 2*, we compare the total scattering coefficient for a case without BAP ($N_{\text{BAP}} = 0$, S_{opt1}) to that predicted for $N_{\text{BAP}} = 0.01 \text{ cm}^{-3}$ (S_{opt2}), $N_{\text{BAP}} = 0.1 \text{ cm}^{-3}$ (S_{opt3}) and $N_{\text{BAP}} = 1 \text{ cm}^{-3}$ (S_{opt4}). At a typical low number concentration of $N_{\text{BAP}} = 0.01 \text{ cm}^{-3}$, the effect on total scattering coefficient is negligible. At $N_{\text{BAP}} = 0.1 \text{ cm}^{-3}$ the total scattering coefficient increases by 15-18% at $\lambda = 0.3\text{-}1.5 \text{ }\mu\text{m}$ although the number fraction of BAP is only 6%. We also use a higher concentration ($N_{\text{BAP}} = 1 \text{ cm}^{-3}$) to explore the maximum effect as BAP concentrations of this order of magnitude have been observed under haze conditions (Wei et al., 2016).



Total scattering coefficient changes by a factor of 0.5-2 depending on λ . Note that the concentration of other particles (N_{other}) would usually increase under haze conditions while we keep N_{other} as a constant in the above
330 model (1.4 cm^{-3}); therefore, the predicted increase of scattering coefficient is clearly the upper limit of the BAP effect. The absorption coefficient of the total aerosol population does not change.

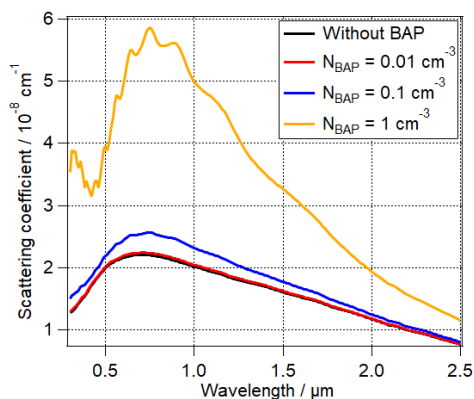
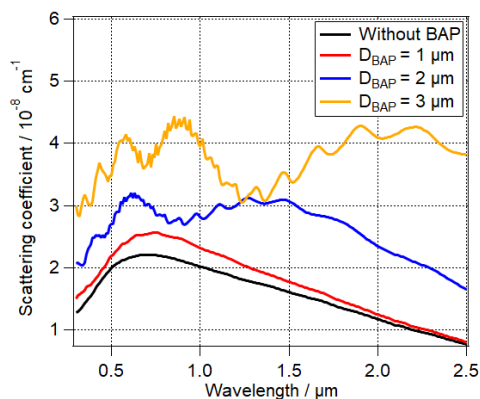


Figure 2. Influence of BAP concentration on total scattering coefficient. The detailed input parameters can be found in **Table 2**. The black line, red line, blue line, and brown line correspond to $S_{\text{opt}1}$, $S_{\text{opt}2}$, $S_{\text{opt}3}$, and $S_{\text{opt}4}$ in **Table 2**, respectively.
335

D_{BAP} also affects the scattering coefficient of the aerosol population significantly (**Figure 3**). $D_{\text{BAP}} = 1 \mu\text{m}$ ($S_{\text{opt}3}$) and $D_{\text{BAP}} = 2 \mu\text{m}$ ($S_{\text{opt}5}$) can be considered to represent different BAP types such as bacteria and fungi, respectively, or an aged bacteria cell that has undergone processing by cell generation (Ervens and Amato,
340 2020). For these assumptions, the scattering coefficient increases depending on λ , with the largest changes of 73-100% at $\lambda > 1.5 \mu\text{m}$ when D_{BAP} increases from $1 \mu\text{m}$ to $2 \mu\text{m}$ ($S_{\text{opt}5}$). Larger BAP ($D_{\text{BAP}} = 3 \mu\text{m}$, $S_{\text{opt}6}$) such as pollen fragments show lead to an increase in the scattering coefficient by a factor of 1.4-4.7 depending on λ . The absorption coefficient of the aerosol population remains nearly the same.

The results in **Figure 3** clearly show that the size of BAP needs to be known in order to assess their optical
345 properties. Even a relatively small variation in particle diameter from 1 to $2 \mu\text{m}$ due to different BAP types or to cell size changes (ΔD_{BAP}) might lead to change in scattering coefficient by 8-100 % depending on λ . Given that the diameter (D_{BAP}) might vary by four orders of magnitude among different BAP types, our analysis shows that different sizes for the various BAP types need to be taken into account if their optical properties are evaluated.



350

Figure 3. Influence of BAP diameter on (a) scattering coefficient and (b) absorption coefficient of total particles. The detailed input parameters can be found in Table 2. The black line, red line, blue line, and brown line correspond to Sopt1, Sopt3, Sopt5, and Sopt6, respectively.

In our model studies, we make the simplistic assumption of spherical BAP particles. Electron scanning
355 microscopic imaging has shown that BAP are not spherical but exhibit a variety of different shapes (Valsan
et al., 2015; Wittmaack et al., 2005). The consequences of the assumptions of spherical versus non-spherical
pollen on the derivation of optical properties at wavelength of 0.65 μm have been recently discussed (Liu
and Yin, 2016). The extinction efficiency (sum of scattering efficiency and absorption efficiency) can vary
by a factor of one to three for small pollen with $D < 4 \mu\text{m}$. For larger pollen with $D > 5 \mu\text{m}$, the extinction
360 efficiency varies by $\sim 25\%$ (Liu and Yin, 2016). While we do not explore sensitivities of BAP geometry, it
may be postulated that under atmospheric conditions, i.e. when BAP are wet, they are more spherical than
under the experimental dry conditions, and thus effects due to non-sphericity may be reduced.

4.1.2 Influence of hygroscopicity (κ_{BAP}) and surface tension (σ_{BAP}) on scattering and absorption

As discussed in *Section 2.3*, g_{BAP} might vary depending on BAP hygroscopicity (κ_{BAP}) and surface tension
365 (σ_{BAP}). **Figure 4** shows the influence of κ on scattering and absorption at RH of 10% ($S_{\text{opt}7}$, $S_{\text{opt}8}$) and 90%
($S_{\text{opt}9}$, $S_{\text{opt}10}$). At RH = 10% ($S_{\text{opt}7}$, $S_{\text{opt}8}$), the influence of BAP on scattering coefficient of total particles is
small ($< 19\%$) and the influence on absorption coefficient is negligible. Assuming $\kappa = 0.25$ ($S_{\text{opt}10}$) instead
of $\kappa = 0.03$ ($S_{\text{opt}9}$), leads to an increase of the scattering coefficient by 17-90% at RH = 90%. Also the
absorption coefficient increases by $\sim 40\%$ at $\lambda > 2 \mu\text{m}$. It can be concluded that the importance of $\Delta\kappa$
370 increases for higher RH as under these conditions BAP hygroscopic growth is most efficient.

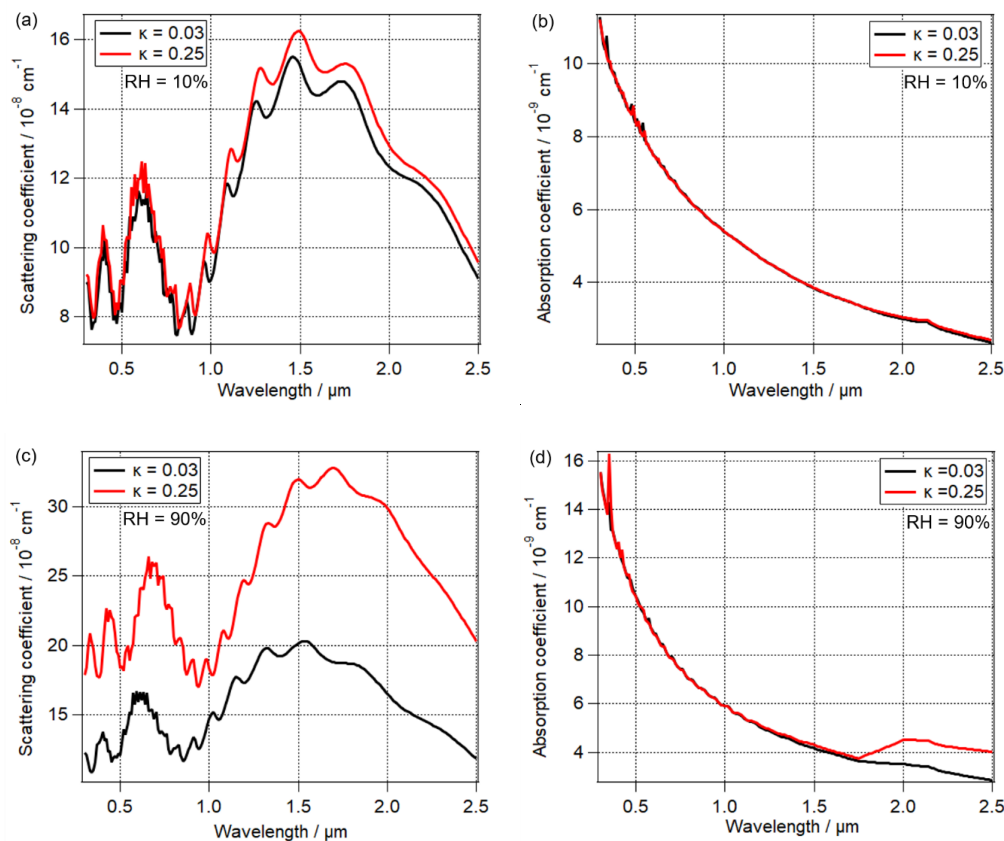


Figure 4. The effect of BAP hygroscopicity (κ) on (a) scattering coefficient, (b) absorption coefficient of total particles at RH = 10% (Sopt7, Sopt8), and RH = 90% (Sopt9, Sopt10).

In addition to hygroscopicity (κ_{BAP}), we explore the importance of biosurfactants which decrease surface tension of particles (σ_{BAP}). A lower surface tension leads to a reduced particle curvature which, in turn, enhances the water uptake. Numerically, this is expressed in the Köhler equation, which can be generally expressed as **Equation 2**:

$$s = \exp\left(\frac{A(\sigma)}{D_{\text{wet}}} - \frac{B(\kappa)}{D_{\text{wet}}^3}\right) \quad (2)$$

where s is the equilibrium water vapor saturation ratio, D_{wet} the wet particle diameter, the first term in the parentheses is the Kelvin (curvature) term which is a function of surface tension (σ_{BAP}) following **Equation 3** and the second term is the Raoult (solute) term which can be parameterized by κ_{BAP} (Rose et al., 2008) following **Equation 4**:

$$\text{Kelvin term} = \frac{A(\sigma)}{D_{\text{wet}}} = \frac{4\sigma_{\text{sol}}M_{\omega}}{\rho_{\omega}RTD_{\text{wet}}} \quad (3)$$



$$\text{Raoult term} = \frac{B(\kappa)}{D_{\text{wet}}^3} = -\ln \frac{D_{\text{wet}}^3 - D_s^3}{D_{\text{wet}}^3 - D_s^3(1-\kappa)} \quad (4)$$

where σ_{sol} is surface tension of solution droplet (72 mN m^{-1}); M_w is molar mass of water (18 g mol^{-1}); ρ_w is density of water (1 g cm^{-3}); R is the universal gas constant ($8.31 \cdot 10^7 \text{ g cm}^2 \text{ s}^{-2} \text{ K}^{-1} \text{ mol}^{-1}$); T is the absolute temperature (K); D_{wet} is droplet diameter (cm); and D_s is the diameter of dry solute particle (cm).

The comparison of the two dimensionless terms shows that in most of the cases, the Raoult term exceeds the Kelvin term by at least one order of magnitude. Only for very small BAP, i.e. representative for viruses or bacteria fragments (*Section 2.1*), the curvature term significantly influences s (*Figure 5*). Based on this analysis, we can conclude that (bio)surfactants likely do not have a significant impact on the hygroscopic growth of BAP. A coating with surfactants might slow down the kinetics of the water uptake by particles (Davidovits et al., 2006). However, since the growth time scales of particles at $\text{RH} < 100\%$ are usually relatively long, the impact of surfactants on the time scale to reach equilibrium sizes is likely small, leading to a small importance of the effect of surfactant on water uptake and the corresponding optical properties.

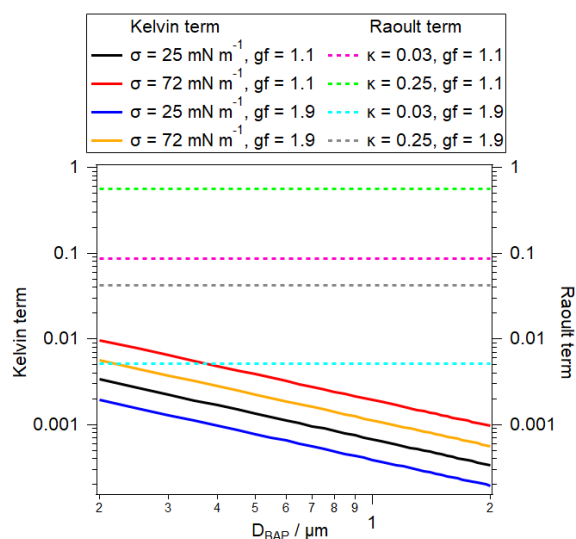


Figure 5. Kelvin term as a function of surface tension (σ_{BAP}) for the σ range as found for BAP (left axis; solid lines). Raoult term as a function of hygroscopicity (κ_{BAP}) for the range of κ as found for BAP (right axis; dashed lines).

4.1.3 Influence of complex refractive index ($m_{\text{BAP}} = n + ik$) on scattering and absorption

The complex refractive index of BAP can be explained by their building blocks of various functional groups (Hill et al., 2015). Hu et al. (2019) have measured the complex refractive indices of 12 types of BAP including bacteria, pollen, and spores. Here we use *Bacillus subtilis* bacteria and *Lactobacillus acidophilus*



bacteria, *Aspergillus oryzae* fungal spores, and lotus pollen as representative BAP types (**Table 1**) to show how the refractive index of different BAP might affect scattering and absorption coefficients of total particles. The scattering coefficient can vary by a factor of two and the absorption coefficient by a factor of five, depending on the wavelength with the largest effects at $\lambda > 2 \mu\text{m}$ (**Figure 6**).

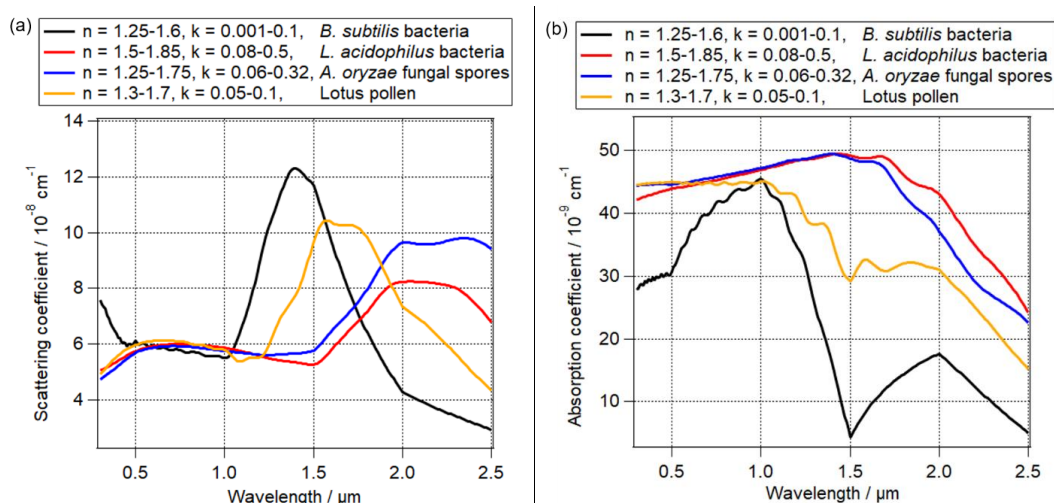


Figure 6. The influence of different types of BAP on (a) the scattering coefficient and (b) absorption coefficient of total particles. The black, red, blue, and brown lines correspond to $S_{\text{opt}11}$, $S_{\text{opt}12}$, $S_{\text{opt}13}$, and $S_{\text{opt}14}$, respectively. All of other parameters are assumed to be equal (i.e. D_{BAP} , N_{BAP} , K_{BAP} and RH).

In addition to the variability in refractive index due to BAP type, chemical processing of the macromolecules at the BAP surface might modify the refractive index. It has been shown that nitration of SOA, i.e. the addition of a nitro group, leads to the formation of brown carbon (Moise et al., 2015). Qualitatively, it has been demonstrated that proteins can be nitrated, similar to SOA compounds (Shiraiwa et al., 2012). Due to the lack of data on Δm for nitrated proteins in BAP, we assume a similar change in the refractive index as in SOA ($S_{\text{opt}13}$ and $S_{\text{opt}14}$). The scattering coefficient can change by up to 20% and the absorption coefficient by a factor of three at $\lambda = 0.42 \mu\text{m}$ (**Figure 7**). Thus, the variability in scattering/absorption properties of BAP due to Δm caused by nitration is likely smaller than due to Δm caused by different BAP types. The assumptions on Δm made for the simulations shown in **Figure 7** are likely an overestimate of the chemical processing of proteins as BAP constituents since (1) experimental conditions are often optimized so that a large fraction of particles is nitrated (Liu et al., 2015) as opposed to ~0.1% of nitrated proteins observed in the atmosphere (Franze et al., 2005), (2) we assume nitration to occur over the whole residence time of particles in the atmosphere while proteins can be nitrated only under conditions of sufficiently high NO_x levels (Shiraiwa et al., 2012), and (3) a rather high concentration of $N_{\text{BAP}} = 1 \text{ cm}^{-3}$ is considered.

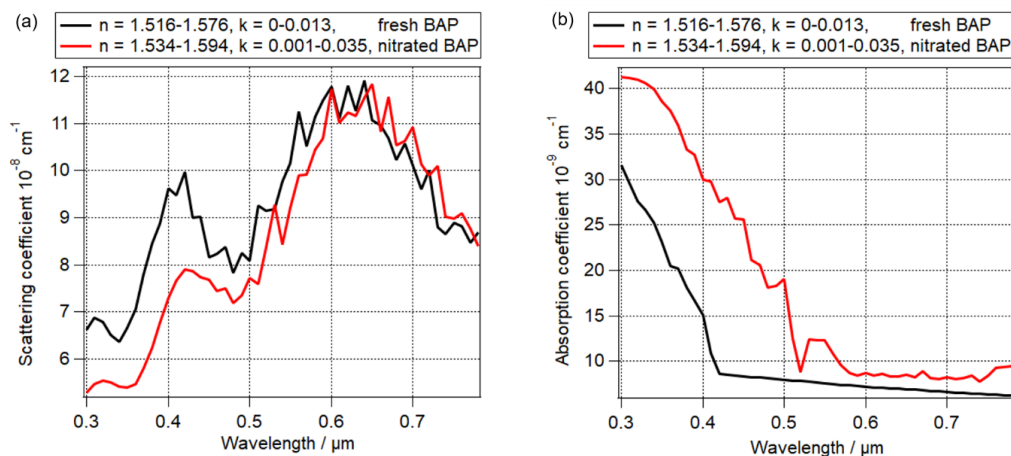


Figure 7. The influence of protein nitration on (a) the scattering coefficient and (b) absorption coefficient of total particles. The black and red correspond to S_{opt15} and S_{opt16} , respectively.

4.1.4 Estimate of change of radiative forcing introduced by BAP

In order to give an estimate of the local radiative forcing due to BAPs, we applied the same approach as Dinar et al. (2007). The radiative forcing efficiency (RFE, i.e. radiative forcing per unit optical depth) at 390 nm can be calculated as:

$$RFE = S_{con} D_{len} (1 - A_{cl}) T_{atm}^2 (1 - R_{sfc})^2 \left[2R_{sfc} \frac{1-\omega}{(1-R_{sfc})^2} - \beta\omega \right] \quad (5)$$

where S_{con} is the solar constant (1370 W m^{-2}); D_{len} is the fractional day length (0.5); A_{cl} is the fractional cloud cover (0.6); T_{atm} is the solar atmospheric transmittance (0.76), and R_{sfc} is surface albedo (0.15); ω is the single scattering albedo (SSA), which is the ratio of scattering coefficient to extinction coefficient; β is average upscatter fraction, which can be calculated as:

$$\beta = 0.082 + 1.85b - 2.97b^2 \quad (6)$$

where b is the ratio of backscattering to scattering coefficient, g is the asymmetry factor which is assumed as 0.65 as an average of ambient measurements ($\sim 0.59-0.72$ (Andrews et al., 2006)). The calculated RFE are listed in **Table 3** for some of the model results of the simulations listed in **Table 2**. The first row is the reference with internally mixed ammonium sulfate/soot particles only while BAP are absent. With a typical concentration of $N_{BAP} = 0.01 \text{ cm}^{-3}$ (S_{opt2}), SSA increases both at $\lambda = 390 \text{ nm}$ and at $\lambda = 532 \text{ nm}$, which means that BAP have a net cooling effect of $\Delta RFE = -0.22 \text{ W m}^{-2}$ at $\lambda = 390 \text{ nm}$ and $\Delta RFE = -0.15 \text{ W m}^{-2}$ at $\lambda = 532 \text{ nm}$, respectively.



Table 3. Radiative forcing efficiency (RFE) at 390 nm and 532 nm calculated based on Equations 7 and 8 for the Mie sensitivity studies. Some typical conditions are shown here to demonstrate the influence of various properties of BAP.

Simulation	SSA	390 nm		532 nm		
		RFE (W m ⁻²)	ΔRFE (W m ⁻²)	RFE (W m ⁻²)	ΔRFE (W m ⁻²)	
S _{opt1} (without BAP, reference)	0.643	-0.5	-	0.728	-6.84	-
S _{opt2} (N _{BAP} = 0.01 cm ⁻³ , D _{BAP} = 1 μm)	0.646	-0.72	-0.22	0.73	-6.99	-0.15
S _{opt3} (N _{BAP} = 0.1 cm ⁻³ , D _{BAP} = 1 μm)	0.668	-2.36	-1.86	0.747	-8.26	-1.42
S _{opt5} (N _{BAP} = 0.1 cm ⁻³ , D _{BAP} = 2 μm)	0.738	-7.59	-7.09	0.791	-11.54	-4.68
S _{opt13} (N _{BAP} = 0.1 cm ⁻³ , D _{BAP} = 2 μm, Δm _{fungalspores})	0.535	7.56	8.06	0.56	5.69	12.53
S _{opt15} (N _{BAP} = 0.1 cm ⁻³ , D _{BAP} = 2 μm, Δm _{freshBAP})	0.852	-16.1	-15.6	0.929	-21.83	-14.99
S _{opt16} (N _{BAP} = 0.1 cm ⁻³ , D _{BAP} = 2 μm, Δm _{agedBAP})	0.692	-4.15	-3.65	0.891	-19	-12.16

455 Note that the RFE values in **Table 3** only represent radiative forcing of a small range of particle sizes and a constant composition and number concentration of other particles; however, the relative differences (ΔRFE) are meaningful and allow evaluating the relative importance of the various BAP parameters (N_{BAP}, D_{BAP}, Δm_{BAP}) in terms of the direct radiative effect. A decrease in RFE implies less absorption, and thus more cooling of atmosphere (Dinar et al., 2007). ΔN_{BAP} (S_{opt3}) and ΔD_{BAP} (S_{opt4}) have a significant influence on
 460 ΔRFE. In addition, ΔRFE at λ = 390 nm is higher than that at λ = 532 nm, implying the increasing importance of BAP in the UV range.

When fungal spores are considered instead of bacteria (i.e., m = n + ik is changed), SSA decreases and RFE even changes from a negative to a positive value (S_{opt13}), resulting in predicted RFE of 7.56 W m⁻² at λ = 390 nm and 5.69 W m⁻² at λ = 532 nm, respectively. This might be explained by the strong light absorption
 465 (very high k) of *Aspergillus oryzae* fungal spores. Generally, the imaginary part k can vary by three orders of magnitude between different types of BAP (**Table 1**), which makes both the sign and the absolute value of the radiative effects of BAP uncertain. Compared to the fresh BAP (S_{opt15}), the cooling effect of nitrated BAP (S_{opt16}) decreases, which can be explained by the increase of k for nitrated BAP due to the formation of brown carbon. These sensitivity studies demonstrate the significant effect of BAP in direct radiative
 470 forcing of supermicron particles. The properties of BAP (e.g. N_{BAP}, D_{BAP}, m_{BAP}) can vary depending on species of BAP and ageing processes. The Largest ΔRFE are caused by Δm_{BAP}.



4.2 Sensitivity of CCN activity to BAP properties

4.2.1 Influence of BAP concentration (N_{BAP}) and diameter (D_{BAP}) on CCN activation

N_{BAP} is low compared to the total CCN concentration (Chow et al., 2015; Sun and Ariya, 2006). The upper
475 limit N_{BAP} is on the order of $\sim 1 \text{ cm}^{-3}$ (**Table 1**) while the number concentration of CCN is usually in the
range of 10s to 1000s cm^{-3} (Ervens et al., 2010). The highest N_{BAP} was found under haze conditions together
with very high total particle concentrations: During haze days in Beijing, N_{BAP} can reach up to $\sim 1.4 \text{ cm}^{-3}$
(Wei et al., 2016) when $N_{\text{CCN}} \sim 10^3 \text{ cm}^{-3}$ (Gunthe et al., 2011). Thus, the ratio of $N_{\text{BAP}} / N_{\text{total}}$ or $N_{\text{BAP}} / N_{\text{CCN}}$
is likely small, i.e. in a range of 0.01-0.14%, independent of location. While such a marginal increase in the
480 number concentration of cloud droplets does not lead to an observable change in cloud properties, the
properties related to the CCN activation of BAP should be considered being more important for biological
reasons, i.e. for BAP to be surrounded by water and the significant modification of the atmospheric residence
time of BAP that is consequently changed by the transport and precipitation in clouds.

The critical saturation s_c can be used as a measure to estimate whether a particle will be activated into a
485 cloud droplet (Rose et al., 2008):

$$s_c = \exp\left(\sqrt{\frac{4A^3}{27\kappa D_s^3}}\right) \quad (7)$$

where A can be found at **Equation 5**, κ is hygroscopicity, and D_s (cm) is mass equivalent diameter of dry
solute particle. Applying this equation, one finds that for particles with $D_{\text{BAP}} = 0.01\text{--}10 \text{ }\mu\text{m}$, the critical
supersaturations ($S_c = (s_c - 1) \cdot 100\%$) are in a broad range of 0.0007%-24% (assuming $\kappa = 0.03$; $\sigma = 72 \text{ mN}$
490 m^{-1}). For large BAP with $D_{\text{BAP}} > 0.5 \text{ }\mu\text{m}$, the critical supersaturations S_c is smaller than 0.062%. Typical
supersaturations (S_{env}) in stratocumulus and convective cumulus clouds are in the range of $\sim 0.1\text{--}0.5\%$ and
 $\sim 0.5\text{--}1\%$, respectively (Pruppacher and Klett, 1997). Comparison to $S_{c,\text{BAP}}$ shows that most BAP ($D_{\text{BAP}} > 0.5$
 μm) are likely activated in clouds as their S_c are significantly smaller than S_{env} in clouds.

4.2.2 Influence of the hygroscopicity (κ_{BAP}) and surface tension (σ_{BAP}) on CCN activation

Figure 8a shows the range of S_c for the κ values shown in **Table 2** for the smallest BAP with $D_{\text{BAP}} = 500$
495 nm, 100 nm, and 50 nm. For $D_{\text{BAP}} = 500 \text{ nm}$, S_c is 0.02% ($\kappa_{\text{BAP}} = 0.25$, S_{CCN1}) or 0.06% ($\kappa_{\text{BAP}} = 0.03$, S_{CCN2}),
which are both below typical S_{env} in clouds. Only for smaller BAP such as bacterial fragments or viruses
with $D_{\text{BAP}} = 100 \text{ nm}$ (S_{CCN3} , S_{CCN4}), S_c changes from 0.24% (S_{CCN3}) to 0.69% (S_{CCN4}) when $\Delta\kappa_{\text{BAP}} = 0.22$.
For even smaller D_{BAP} (50 nm), S_c increases from 0.68% (S_{CCN5}) to 1.97% (S_{CCN6}) when $\Delta\kappa_{\text{BAP}} = 0.22$. Thus,
500 only for fairly small BAP, the hygroscopicity κ_{BAP} may impact their CCN activation.

Overlaid on the vertical lines for S_c in **Figure 8a** are S_{env} in the cloud as calculated in our parcel model for
different updraft velocities ($w = 10 \text{ cm s}^{-1}$, 100 cm s^{-1} , and 300 cm s^{-1}). The sensitivity of CCN properties to



updraft velocity and S_{env} has been discussed in numerous previous studies, e.g., Ervens et al. (2005, 2007). **Figure 8a** corroborates the conclusions from these previous studies that the variation of the κ over wide
 505 ranges only introduces a small change in the CCN activity and in cloud properties (e.g., drop number concentration, LWC) and that particle composition is most important in clouds with low updraft velocities.

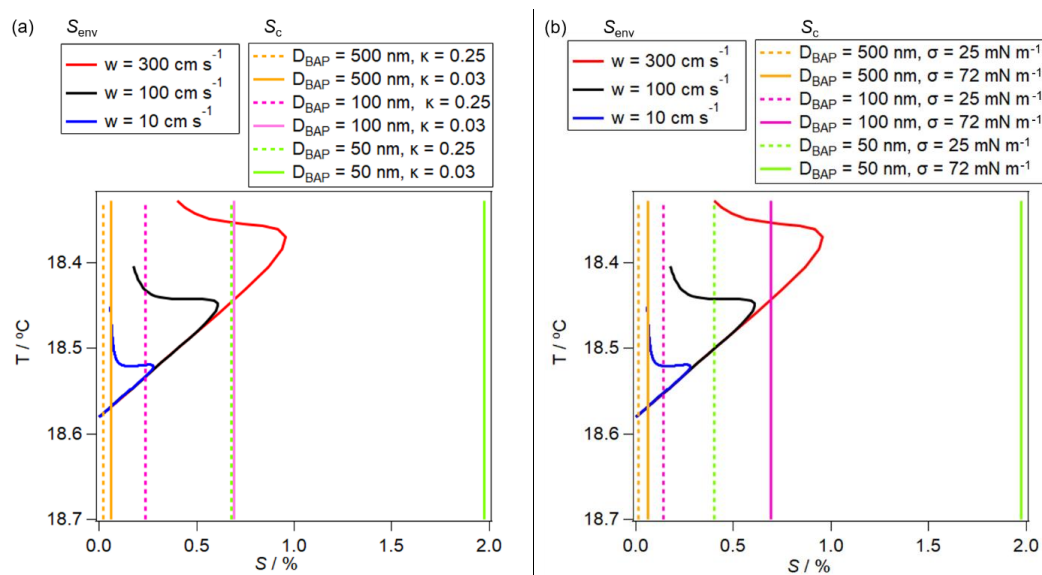


Figure 8. Comparison of S_{env} to S_c of BAP with (a) different κ or (b) different σ . Model details can be found in **Table 2**.

510 Similar to S_c ranges due to different κ_{BAP} values, we compare in **Figure 8b** predicted S_c ranges due to different values of σ_{BAP} for high biosurfactant concentrations (when mass fraction of surfactants to total particle mass $> 0.1\%$, $\sigma_{BAP} = 25 \text{ mN m}^{-1}$) to those predicted for very low surfactant concentrations ($\sigma_{BAP} = 72 \text{ mN m}^{-1}$). For BAP with $D_{BAP} = 500 \text{ nm}$, S_c changes from 0.01% (S_{CCN7} , $\sigma_{BAP} = 25 \text{ mN m}^{-1}$) to 0.06% (S_{CCN2} , $\sigma_{BAP} = 72 \text{ mN m}^{-1}$). As discussed before, these large BAP will be likely all activated in clouds and
 515 the small difference in S_c introduced by $\Delta\sigma$ does not cause a difference in their CCN ability. For smaller BAP, such as bacterial fragments or viruses with $D_{BAP} = 100 \text{ nm}$, S_c changes from 0.14% (S_{CCN8}) to 0.69% (S_{CCN4}) when $\Delta\sigma_{BAP} = 47 \text{ mN m}^{-1}$. When D_{BAP} further decreases to 50 nm, S_c changes from 0.4% (S_{CCN9}) to 1.97% (S_{CCN6}) when $\Delta\sigma_{BAP} = 47 \text{ mN m}^{-1}$. Therefore, the effect of biosurfactant needs to be considered for
 520 small BAP in terms of CCN activity if a sufficiently large mass fraction of strongly surface-active biosurfactant is present. Note that the assumption of $\sigma_{BAP} = 25 \text{ mN m}^{-1}$ in **Figure 8b** likely represents an overestimate as most biosurfactants exhibit a range of $30 \text{ mN m}^{-1} < \sigma_{BAP} < 55 \text{ mN m}^{-1}$ (Renard et al., 2016). In addition, the biosurfactant concentration, and thus the surface tension according to **Equation 1**, depends



on the mass fraction of biosurfactants in the BAP, the growth factor and on diameter of BAP. If the mass fraction is very low, $\sigma_{\text{BAP}} = 72 \text{ mN m}^{-1}$; when the mass fraction of biosurfactants approaches $\sim 0.1\%$, σ_{BAP} might be as low as 25 mN m^{-1} . Typical surfactant mass concentrations are on the order of $\sim 0.1\%$ (Gérard et al., 2019); mass fractions for specific biosurfactants have not been determined yet. Such low mass fraction implies that only a few ($< 10\text{--}100$) surfactant molecules (with a molecular weight $M \sim 1000 \text{ g mol}^{-1}$) are present on submicron particles and/or that only a fraction of particles is completely covered by surfactants and thus exhibits a reduced surface tension. While biosurfactants might be also taken up by other particles while they reside on surfaces (soil, vegetation) where BAP were active, our conclusions also hold for such particles. Our sensitivity studies show once more that under dynamic conditions in clouds buffering reduces the feedbacks of particle composition on supersaturation (Ervens et al., 2005; Stevens and Feingold, 2009). Therefore, previous estimates of surfactant effects on cloud properties that are based on a simplified assumption of equilibrium conditions in clouds (Facchini et al., 1999), led to an overestimate of the role of surfactants on CCN.

We conclude that the mass concentration of biosurfactants needs to be quantified in order to better explore the biosurfactant effect on CCN activation of small particles. Given that the surface concentration of surfactants is likely higher than the bulk concentration (Bzdek et al., 2020; Lowe et al., 2019; Ruehl et al., 2016) as assumed here, even a smaller mass fraction of biosurfactants than calculated by *Equation 1* might be sufficient to decrease the surface tension of small aqueous BAP and the corresponding critical supersaturation. However, also for the concept of surface partitioning of biosurfactants, rather than for a bulk concentration, our conclusions hold true on the limited impact of surface tension suppression on CCN activation of supermicron BAPs.

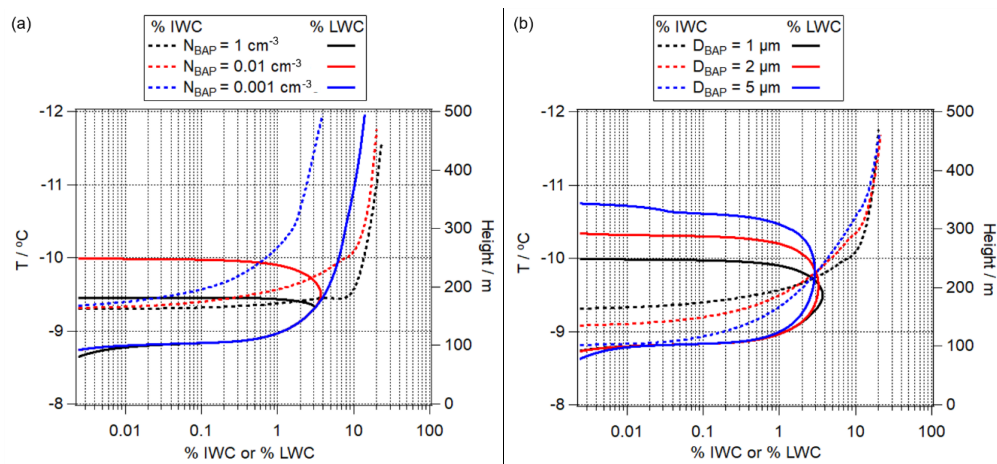
4.3 Sensitivity of mixed-phase cloud evolution to BAP properties

4.3.1 Influence of BAP concentration (N_{BAP}) and diameter (D_{BAP}) on ice nucleation

N_{BAP} is on the same order of magnitude as that of total IN in some regions and at temperatures $T > \sim -10^\circ\text{C}$ (Pratt et al., 2009; Prenni et al., 2009), which makes BAP play an important role in mixed-phase clouds. Especially, at these relatively high temperatures, some bacteria and fungi species can nucleate ice while other particles cannot, and therefore $N_{\text{BAP, IN}} / N_{\text{IN}}$ is $\sim 100\%$. *Figure 9a* shows the change of ice water content (IWC, solid lines) and liquid water content (LWC, dashed lines) in a mixed-phase cloud (S_{IN1} , S_{IN2} , S_{IN3}). Above an IWC of $\sim 3\%$, ice particles start growing at the expense of liquid water (Bergeron-Findeisen-Process) (S_{IN1}). At lower $N_{\text{BAP}} \sim 0.01 \text{ cm}^{-3}$ (S_{IN2}), the onset of the Bergeron-Findeisen-Process starts slightly later. With $N_{\text{BAP}} \sim 0.001 \text{ cm}^{-3}$ (S_{IN3}), both IWC and LWC are predicted to increase simultaneously throughout the whole cloud, i.e. the Bergeron-Findeisen-Process is not initiated and cloud glaciation does not take place.



555 In **Figure 9b**, we compare model results for simulations S_{IN4} and S_{IN5} in order to explore the effect of D_{BAP} .
With larger BAP size such as $D_{BAP} = 2 \mu\text{m}$ (S_{IN4}) or $D_{BAP} = 5 \mu\text{m}$ (S_{IN5}), ice formation starts earlier in the
cloud, but the onset of the Bergeron-Findeisen process occurs at approximately the same temperature as for
smaller D_{BAP} because of the feedbacks of IWC and LWC on the supersaturations in the cloud and vice versa.
In agreement with previous sensitivity studies (Ervens et al., 2011; Ervens and Feingold, 2013), these results
560 confirm that the influence of D on the IN activity is relatively small (**Figure 9**). Based on these trends, it
can be also concluded that processes that change the BAP size (e.g. ΔD_{BAP} by cell generation) are not critical
to be included in models to represent the variability of IN property effect on mixed-phase clouds.



565 **Figure 9.** Ice water content (IWC, solid lines) and liquid water content (LWC, dashed lines) as a function of (a) N_{BAP} and (b) D_{BAP} . Details on the simulations can be found in **Table 2**.

4.3.2 Influence of the contact angle (θ_{BAP}) on ice nucleation

Different types of BAPs exhibit a wide range of contact angles of $4^\circ < \theta_{BAP} < 44^\circ$ (**Table 1** and **Section 2**).
As shown in **Figure 10**, different BAP types that have θ_{BAP} of 4° or 20° , respectively, lead to a difference
570 in temperature, at which the Bergeron-Findeisen process occurs, by $\Delta T \sim 0.6^\circ\text{C}$. For BAP with even higher
 θ_{BAP} (40°), the Bergeron-Findeisen process occurs even at a lower temperature ($\Delta T \sim 3.3^\circ\text{C}$).

As discussed in **Section 2**, chemical (e.g., nitration, oxidation, adjustments due to pH) or physical processing
of IN surfaces might lead to $\Delta\theta_{BAP} \sim 1^\circ$. In **Figure 10d**, we show the resulting change in IWC and LWC
575 evolution by comparing S_{IN2} and S_{IN9} . It is clear that even such a small change in θ can cause a significant
difference in the IWC and LWC evolutions. The temperature, at which the Bergeron-Findeisen process
occurs differs by $\Delta T \sim 1.3^\circ\text{C}$. These results suggest that a small change of contact angle due to different
types of BAP or due to processing ($\Delta\theta$) might affect the Bergeron-Findeisen process significantly. We only
exemplarily explore $\Delta\theta$ for nitration based on the experiments by Attard et al. (2012). In the same study, it



580 was found that $\Delta\theta$ is $\sim 1.5^\circ$ for bacteria such as *Pseudomonas syringae* when the cells were exposed to solutions of pH 7.0 and 4.1 at temperatures of $T > -10^\circ\text{C}$.

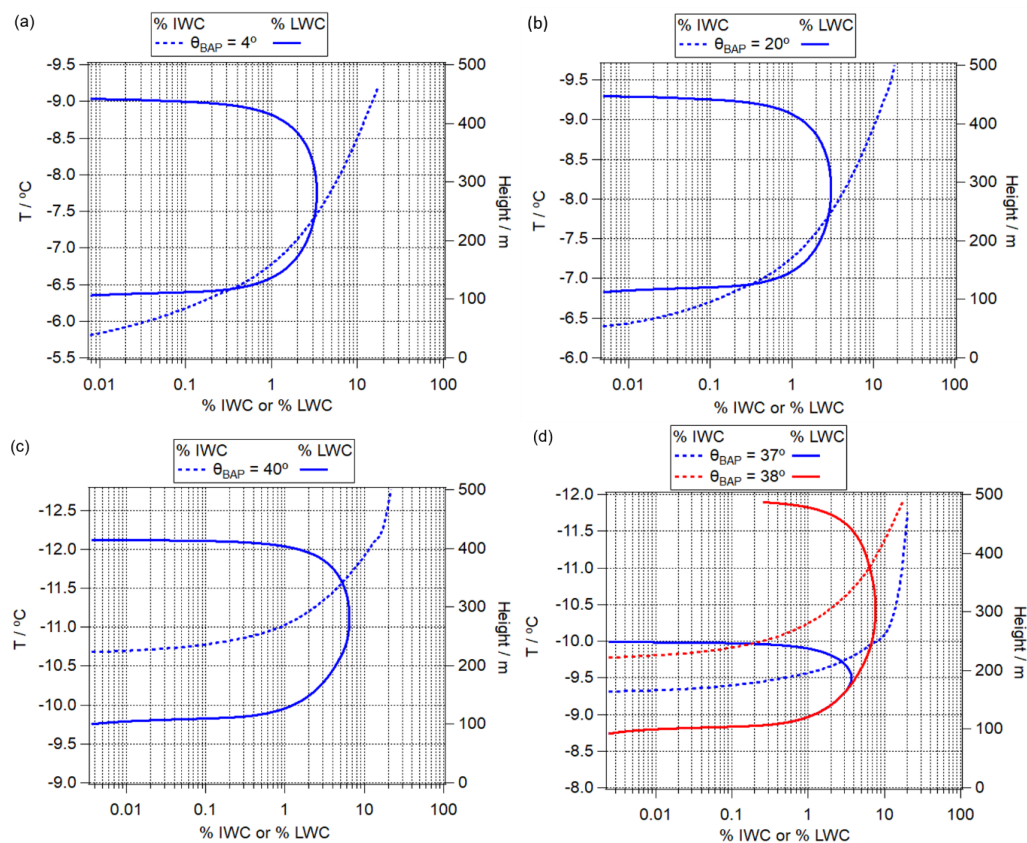


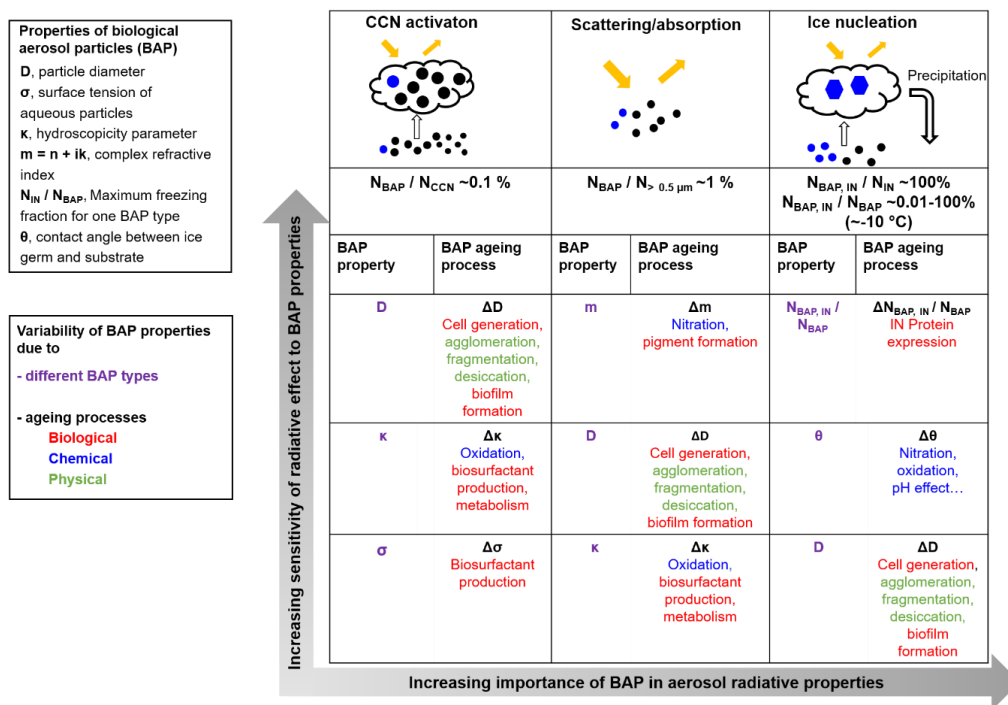
Figure 10. Ice water content (IWC, solid lines) and liquid water content (LWC, dashed lines) as a function of θ_{BAP} . Even when the contact angle increases by 1° , the initiation of Bergeron-Findeisen process might be influenced significantly.

585 Similar exercises could be done for differences in θ due to other processes, such as the oxidation of pollen
that lead to $\Delta\theta \sim 1.5^\circ$ at $T \sim -39^\circ\text{C}$ (Gute and Abbatt, 2018). However, at this much lower temperature, the
sensitivity of the frozen fraction to $\Delta\theta$ decreases (Ervens and Feingold, 2013). Overall, it can be concluded
that chemical processing of bacteria or other BAP that freeze at relatively high temperatures in the
atmospheric for extended periods of time might sufficiently alter their surface to induce a significant change
590 in their IN ability.



5. Conclusions

Based on our model sensitivity studies, we can rank the importance of the various parameters and processes of BAPs shown in *Figure 1* in terms of their radiative effects: The increasing importance and sensitivity are summarized in *Figure 11*.



595

Figure 11. Schematic of the importance of BAP in the climate system and the sensitivity of radiative effect to BAP properties. The bottom arrow shows the increasing importance of BAP in CCN, scattering/absorption, and IN. The left arrow indicates the increasing sensitivity to BAP properties, which depend on the type of BAP and ageing processes.

600

As the number concentration of BAPs only contribute $\sim 0.1\%$ to the total CCN concentration, even under conditions of high N_{BAP} , their role in CCN activation in warm clouds is negligible as they do not lead to any significant change in cloud properties. Since BAPs have usually supermicron sizes, they will act as CCN and even small changes in their chemical composition do not affect their CCN activity. The CCN activation of smaller BAPs such as bacteria fragments or viruses might be influenced by their hygroscopicity (K_{BAP}) and surface tension (σ_{BAP}). K_{BAP} might be modified by chemical (e.g., nitration, oxidation), physical (e.g., condensation of gases), and biological processes (e.g., formation of metabolic products, biosurfactants). Biosurfactants decrease the surface tension of BAPs (σ_{BAP}) and possibly even of other particles (σ_{other}) to

605



increase their CCN ability. Even though the CCN activation of BAPs might be of very limited importance
610 for cloud properties, it is more important due to biological aspects as it is a survival strategy of
microorganisms to improve their environmental conditions by water uptake, drop formation, and spreading
on hydrophobic surfaces to enhance their survival time in the biosphere and atmosphere.

BAPs contribute ~1% to large particles with $D > 0.5 \mu\text{m}$, which makes them relatively important for the
aerosol direct effect. BAPs have a direct cooling effect for most properties explored here whereas they could
615 also change to a direct warming effect for certain species of BAPs. The most sensitive BAP property is the
complex refractive index ($m = n + ik$), especially the imaginary part (k) which varies by three orders of
magnitude among different types of BAPs. Assuming, for example, that all BAPs have the optical properties
of *Aspergillus oryzae* fungal spores, the predicted direct aerosol effect changes from a cooling to a warming
effect. Our RFE estimates clearly represent an overestimate as we only consider a small particle size range
620 and concentration. Thus, the identified relative changes in RFE due to different BAP types and properties
should be considered more representative than the absolute numbers.

The complex refractive index m_{BAP} can be modified due to chemical or biological processing. For example,
nitration could lead to an enhancement of the imaginary part (absorptive properties), but the difference of
scattering and absorption coefficient induced by nitration is much smaller compared to the differences
625 caused by the refractive indices of different BAP types. Biological processing such as pigment formation
(Pšenčík et al., 2004; Fong et al., 2001) might also lead to Δm_{BAP} to a significant extent, but we cannot
quantify the role of this process in our model framework due to the lack of corresponding data. The second
ranked parameter is ΔD_{BAP} , which also differs among different types of BAP or might change for one BAP
type due cell generation or desiccation in the atmosphere. Obviously, the total number of BAP (N_{BAP}) is
630 of importance for all effects discussed here. However, as it has been shown that at many location $N_{\text{BAP}}/N_{\text{total}}$
is approximately constant, the relative role of BAP likely does not change due to differences in absolute
BAP concentration. Hygroscopicity κ might have an effect under high RH conditions. The effect of surface
tension σ on direct radiative property is negligible.

The most important role of BAP is to act as IN because $N_{\text{BAP, IN}}/N_{\text{IN}}$ can reach up to ~100% at $T > -10 \text{ }^\circ\text{C}$.
635 Given the high sensitivity of BAPs that initiate freezing, it is clear that not only the total N_{BAP} but also the
fraction that can freeze needs to be constrained. While this fraction is usually ~100% for pollen, it can be as
small as 0.01%-10% for bacteria. As identified in previous sensitivity studies, the surface composition
properties, often expressed in terms of a contact angle θ_{BAP} , shows the highest importance to IN activity and
therefore to the evolution of mixed-phase clouds (Bergeron-Findeisen process). The variability of θ_{BAP}
640 between different types of BAP ($4^\circ < \theta_{\text{BAP}} < 44^\circ$) determines the onset temperature of freezing and the
temperature interval in which the Bergeron Findeisen process may occur. Even a small change of $\Delta\theta_{\text{BAP}} \sim 1^\circ$



as caused by chemical processing on BAP surfaces or pH change might affect the onset of the Bergeron-Findeisen process significantly. Thus, not only various BAP types should be parameterized with different θ_{BAP} in models but also $\Delta\theta_{\text{BAP}}$ due to modification by chemical and possibly biological processes.

645 The trends discussed above are summarized in **Figure 11** and show the relative importance of BAPs in the atmosphere, increasing from their roles in CCN activation, to the aerosol direct effect and to mixed-phase cloud evolution. The arrows on the left and on the bottom point to the most sensitive and most important parameters, respectively, which are placed in the upper right corner of the table.

Our study highlights the possible importance of BAP processing as not only chemical and physical processes
650 but also biological ageing processes can modify the chemical composition and physical properties of BAPs. While the former two process types commonly occur on/in many other ambient particles as well (e.g. Δm due to nitration of SOA, or ΔD due to condensation of low volatility material), biological processing is unique to BAPs and currently not comprehensively included and explored in atmospheric models. For example, we suggest that cell generation or the expression of specific proteins might significantly affect
655 BAP's IN ability. While the role of biosurfactant production ($\Delta\sigma_{\text{BAP}}$) is limited in modulating warm cloud properties and the aerosol direct effect, the biological aspects of this process might be of much larger importance: Enhanced water uptake by BAPs may extend lifetime of the microorganisms by improving their living conditions, i.e. reduce stress due to harsh ambient conditions (e.g. high ionic strength, low pH, desiccation). In addition, their inclusion in clouds as IN or CCN will lead to a more efficient transport and
660 distribution across the atmosphere.

In addition to the few biological processes discussed in our study, additional biological processes (e.g., pigment formation, carotenoid accumulation, formation of metabolic products, biofilm formation) are included in **Figure 11** to give a more complete picture of ageing processes of BAP that may affect their radiative properties. Several of our results repeat findings from previous sensitivity studies of aerosol
665 properties on the direct and indirect radiative effects. However, our study should be considered as guidance to future field, lab and model studies to further characterize the role of biological particles in the atmosphere as their emissions, budgets and processing are currently poorly constrained (Khaled et al., 2020) compared to more abundant aerosol types, despite their unique characteristics of living organisms that may affect not only climate but also public health.

670 **Code and data availability:** Details on the model codes and further model results can be obtained from the corresponding author upon request.

Author contributions: MZ and BE designed the model framework. AK, PA, AD contributed by fruitful discussions and commented on the manuscript.



Competing interests: The authors declare that they do not have any competing interests.

675 **References**

- Akbari, S., Abdurahman, N. H., Yunus, R. M., Fayaz, F. and Alara, O. R.: Biosurfactants—a new frontier for social and environmental safety: a mini review, *Biotechnol. Res. Innov.*, 2, 81–90, <https://doi.org/10.1016/j.biori.2018.09.001>, 2018.
- Amato, P., Joly, M., Besaury, L., Oudart, A., Taib, N., Moné, A. I., Deguillaume, L., Delort, A. M. and
680 Debroas, D.: Active microorganisms thrive among extremely diverse communities in cloud water, *PLoS One*, 12, e0182869, <https://doi.org/10.1371/journal.pone.0182869>, 2017.
- Andrews, E., Sheridan, P. J., Fiebig, M., McComiskey, A., Ogren, J. A., Arnott, P., Covert, D., Elleman, R., Gasparini, R., Collins, D., Jonsson, H., Schmid, B. and Wang, J.: Comparison of methods for deriving aerosol asymmetry parameter, *J. Geophys. Res. Atmos.*, 111, D5, <https://doi.org/10.1029/2004JD005734>, 2006.
- 685 Myhre, G., Shindell, D., Bréon, F. M., Collins, W., Fuglestedt, J., Huang, J., et al. Anthropogenic and Natural Radiative Forcing – in *Climate Change 2013: the Physical Science Basis. Contribution of Working Group I to the Fifth Assessment Report of the Intergovernmental Panel on Climate Change*. Cambridge University Press, 10 <https://doi.org/10.1017/CBO9781107415324> (2013).
- Arakawa, E. T., Tuminello, P. S., Khare, B. N. and Milham, M. E.: Optical properties of *Erwinia herbicola*
690 bacteria at 0.190–2.50 μm , *Biopolym. - Biospectroscopy Sect.*, 72, 391–398, <https://doi.org/10.1002/bip.10438>, 2003.
- Ariya, P. A., Sun, J., Eltouny, N. A., Hudson, E. D., Hayes, C. T. and Kos, G.: Physical and chemical characterization of bioaerosols - Implications for nucleation processes., 28, 1–32, <https://doi.org/10.1080/01442350802597438>, 2009.
- 695 Asadi, S., Bouvier, N., Wexler, A. S. and Ristenpart, W. D.: The coronavirus pandemic and aerosols: Does COVID-19 transmit via expiratory particles?, 54, 635–638, *Aerosol Sci. Technol.*, <https://doi.org/10.1080/02786826.2020.1749229>, 2020.
- Attard, E., Yang, H., Delort, A. M., Amato, P., Pöschl, U., Glaux, C., Koop, T. and Morris, C. E.: Effects of atmospheric conditions on ice nucleation activity of *Pseudomonas*, *Atmos. Chem. Phys.*, 12, 10667–
700 10677, <https://doi.org/10.5194/acp-12-10667-2012>, 2012.
- Ayerst, G.: The effects of moisture and temperature on growth and spore germination in some fungi, *J. Stored Prod. Res.*, 5, 127–141, [https://doi.org/10.1016/0022-474X\(69\)90055-1](https://doi.org/10.1016/0022-474X(69)90055-1), 1969.
- Barahona, D., West, R. E. L., Stier, P., Romakkaniemi, S., Kokkola, H. and Nenes, A.: Comprehensively accounting for the effect of giant CCN in cloud activation parameterizations, *Atmos. Chem. Phys.*, 10, 2467–



- 705 2473, <https://doi.org/10.5194/acp-10-2467-2010>, 2010.
- Barnard, R. L., Osborne, C. A. and Firestone, M. K.: Responses of soil bacterial and fungal communities to extreme desiccation and rewetting, *ISME J.*, 7, 2229–2241, <https://doi.org/10.1038/ismej.2013.104>, 2013.
- Bauer, H., Giebl, H., Hitzenberger, R., Kasper-Giebl, A., Reischl, G., Zibuschka, F. and Puxbaum, H.: Airborne bacteria as cloud condensation nuclei, *J. Geophys. Res. D Atmos.*, 108, 4658
710 <https://doi.org/10.1029/2003jd003545>, 2003.
- Behzad, H., Mineta, K. and Gojobori, T.: Global Ramifications of Dust and Sandstorm Microbiota, *Genome Biol. Evol.*, 10, 1970–1987, <https://doi.org/10.1093/gbe/evy134>, 2018.
- Bohren, C. F., Huffman, D. R.: *Absorption and Scattering of Light by Small Particles*, John Wiley, Hoboken, NJ, USA, 477–482, 1983
- 715 Burrows, S. M., Elbert, W., Lawrence, M. G. and Pöschl, U.: Bacteria in the global atmosphere - Part 1: Review and synthesis of literature data for different ecosystems, *Atmos. Chem. Phys.*, 9, 9263–9280, <https://doi.org/10.5194/acp-9-9263-2009>, 2009a.
- Burrows, S. M., Butler, T., Jöckel, P., Tost, H., Kerkweg, A., Pöschl, U. and Lawrence, M. G.: Bacteria in the global atmosphere - Part 2: Modeling of emissions and transport between different ecosystems, *Atmos. Chem. Phys.*, 9, 9281–9297, <https://doi.org/10.5194/acp-9-9281-2009>, 2009b.
720
- Burrows, S. M., Hoose, C., Pöschl, U. and Lawrence, M. G.: Ice nuclei in marine air: Biogenic particles or dust?, *Atmos. Chem. Phys.*, 13, 245–267, <https://doi.org/10.5194/acp-13-245-2013>, 2013.
- Bzdek, B. R., Reid, J. P., Malila, J. and Prisle, N. L.: The surface tension of surfactant-containing, finite volume droplets, *Proc. Natl. Acad. Sci. U. S. A.*, 117, 8335–8343, <https://doi.org/10.1073/pnas.1915660117>,
725 2020.
- Chen, L., Chen, Y., Chen, L., Gu, W., Peng, C., Luo, S., Song, W., Wang, Z. and Tang, M.: Hygroscopic Properties of 11 Pollen Species in China, *ACS Earth Sp. Chem.*, 3, 2678–2683, <https://doi.org/10.1021/acsearthspacechem.9b00268>, 2019.
- Chow, J. C., Yang, X., Wang, X., Kohl, S. D., Hurbain, P. R., Chen, L. W. A. and Watson, J. G.:
730 Characterization of ambient PM10 bioaerosols in a California agricultural town, *Aerosol Air Qual. Res.*, 15, 1433–1447 <https://doi.org/10.4209/aaqr.2014.12.0313>, 2015.
- Coluzza, I., Creamean, J., Rossi, M. J., Wex, H., Alpert, P. A., Bianco, V., Boose, Y., Dellago, C., Felgitsch, L., Fröhlich-Nowoisky, J., Herrmann, H., Jungblut, S., Kanji, Z. A., Menzl, G., Moffett, B., Moritz, C., Mutzel, A., Pöschl, U., Schauerperl, M., Scheel, J., Stopelli, E., Stratmann, F., Grothe, H. and Schmale, D.
735 G.: Perspectives on the future of ice nucleation research: Research needs and Unanswered questions



- identified from two international workshops, *Atmosphere (Basel)*, 8, 138,
[https://doi:10.3390/atmos8080138](https://doi.org/10.3390/atmos8080138), 2017.
- Davidovits, P., Kolb, C. E., Williams, L. R., Jayne, J. T. and Worsnop, D. R.: Mass accommodation and
chemical reactions at gas-liquid interfaces, *Chem. Rev.*, 106, 1323-1354, [https://doi:10.1021/cr040366k](https://doi.org/10.1021/cr040366k),
740 2006.
- Deguillaume, L., Leriche, M., Amato, P., Ariya, P. A., Delort, A. M., Pöschl, U., Chaumerliac, N., Bauer,
H., Flossmann, A. I. and Morris, C. E.: Microbiology and atmospheric processes: Chemical interactions of
primary biological aerosols, *Biogeosciences*, 5, 1073–1084, [https://doi:10.5194/bg-5-1073-2008](https://doi.org/10.5194/bg-5-1073-2008), 2008.
- DeLeon-Rodriguez, N., Latham, T. L., Rodriguez-R, L. M., Barazesh, J. M., Anderson, B. E., Beyersdorf,
745 A. J., Ziemba, L. D., Bergin, M., Nenes, A. and Konstantinidis, K. T.: Microbiome of the upper troposphere:
Species composition and prevalence, effects of tropical storms, and atmospheric implications, *Proc. Natl.
Acad. Sci. U. S. A.*, 110, 2575-2580, [https://doi:10.1073/pnas.1212089110](https://doi.org/10.1073/pnas.1212089110), 2013.
- Delort, A. M., Vähtilingom, M., Joly, M., Amato, P., Wirgot, N., Lallement, A., Sancelme, M., Matulova,
M. and Deguillaume, L.: Clouds: A transient and stressing habitat for microorganisms, in *Microbial Ecology
750 of Extreme Environments.*, Springer, Cham, Switzerland, 215-245, 2017.
- Després, V., Huffman, J. A., Burrows, S. M., Hoose, C., Safatov, A., Buryak, G., Fröhlich-Nowoisky, J.,
Elbert, W., Andreae, M., Pöschl, U. and Jaenicke, R.: Primary biological aerosol particles in the atmosphere:
a review, *Tellus B Chem. Phys. Meteorol.*, 64, 15598, [https://doi:10.3402/tellusb.v64i0.15598](https://doi.org/10.3402/tellusb.v64i0.15598), 2012.
- Diehl, K., Quick, C., Matthias-Maser, S., Mitra, S. K. and Jaenicke, R.: The ice nucleating ability of pollen
755 Part I: Laboratory studies in deposition and condensation freezing modes, *Atmos. Res.*, 58, 75-87,
[https://doi:10.1016/S0169-8095\(01\)00091-6](https://doi.org/10.1016/S0169-8095(01)00091-6), 2001.
- Diehl, K., Matthias-Maser, S., Jaenicke, R. and Mitra, S. K.: The ice nucleating ability of pollen: Part II.
Laboratory studies in immersion and contact freezing modes, *Atmos. Res.*, 61, 125-133,
[https://doi:10.1016/S0169-8095\(01\)00132-6](https://doi.org/10.1016/S0169-8095(01)00132-6), 2002.
- 760 Dinar, E., Abo Riziq, A., Spindler, C., Erlick, C., Kiss, G. and Rudich, Y.: The complex refractive index of
atmospheric and model humic-like substances (HULIS) retrieved by a cavity ring down aerosol
spectrometer (CRD-AS), *Faraday Discuss.*, 137, 279-295, [https://doi:10.1039/b703111d](https://doi.org/10.1039/b703111d), 2007.
- Enguita, F. J., Martins, L. O., Henriques, A. O. and Carrondo, M. A.: Crystal structure of a bacterial
endospore coat component: A laccase with enhanced thermostability properties, *J. Biol. Chem.*, 278, 19416-
765 19425, [https://doi:10.1074/jbc.M301251200](https://doi.org/10.1074/jbc.M301251200), 2003.
- Ervens, B. and Amato, P.: The global impact of bacterial processes on carbon mass, *Atmos. Chem. Phys.*,



- 20, 1777–1794, <https://doi.org/10.5194/acp-20-1777-2020>, 2020.
- Ervens, B. and Feingold, G.: Sensitivities of immersion freezing: Reconciling classical nucleation theory and deterministic expressions, *Geophys. Res. Lett.*, 40, 3320–3324, <https://doi.org/10.1002/grl.50580>, 2013.
- 770 Ervens, B., Feingold, G. and Kreidenweis, S. M.: Influence of water-soluble organic carbon on cloud drop number concentration, *J. Geophys. Res. D Atmos.*, 110, 1–14, <https://doi.org/10.1029/2004JD005634>, 2005.
- Ervens, B., Cubison, M. J., Andrews, E., Feingold, G., Ogren, J. A., Jimenez, J. L., Quinn, P. K., Bates, T. S., Wang, J., Zhang, Q., Coe, H., Flynn, M. and Allan, J. D.: CCN predictions using simplified assumptions of organic aerosol composition and mixing state: A synthesis from six different locations, *Atmos. Chem. Phys.*, 10, 4795–4807, <https://doi.org/10.5194/acp-10-4795-2010>, 2010.
- 775 Ervens, B., Feingold, G., Sulia, K. and Harrington, J.: The impact of microphysical parameters, ice nucleation mode, and habit growth on the ice/liquid partitioning in mixed-phase Arctic clouds, *J. Geophys. Res. Atmos.*, 116, D17205, <https://doi.org/10.1029/2011JD015729>, 2011.
- Estillore, A. D., Trueblood, J. V. and Grassian, V. H.: Atmospheric chemistry of bioaerosols: Heterogeneous and multiphase reactions with atmospheric oxidants and other trace gases, *Chem. Sci.*, 7, 6604–6616 <https://doi.org/10.1039/c6sc02353c>, 2016.
- 780 Facchini, M. C., Mircea, M., Fuzzi, S. and Charlson, R. J.: Cloud albedo enhancement by surface-active organic solutes in growing droplets, *Nature*, 401, 257–259, <https://doi.org/10.1038/45758>, 1999.
- Feingold, G. and Heymsfield, A. J.: Parameterizations of condensational growth of droplets for use in general circulation models, *J. Atmos. Sci.*, 49, 2325–2342, [https://doi.org/10.1175/1520-0469\(1992\)049<2325:POCGOD>2.0.CO;2](https://doi.org/10.1175/1520-0469(1992)049<2325:POCGOD>2.0.CO;2), 1992.
- 785 Feingold, G., Cotton, W. R., Kreidenweis, S. M. and Davis, J. T.: The impact of giant cloud condensation nuclei on drizzle formation in stratocumulus: Implications for cloud radiative properties, *J. Atmos. Sci.*, 56, 4100–4117, [https://doi.org/10.1175/1520-0469\(1999\)056<4100:TIOGCC>2.0.CO;2](https://doi.org/10.1175/1520-0469(1999)056<4100:TIOGCC>2.0.CO;2), 1999.
- 790 Fong, N. J. C., Burgess, M. L., Barrow, K. D. and Glenn, D. R.: Carotenoid accumulation in the psychrotrophic bacterium *Arthrobacter agilis* in response to thermal and salt stress, *Appl. Microbiol. Biotechnol.*, 56, 750–756, <https://doi.org/10.1007/s002530100739>, 2001.
- Fox, E. M. and Howlett, B. J.: Secondary metabolism: regulation and role in fungal biology, *Curr. Opin. Microbiol.*, 11, 481–487, <https://doi.org/10.1016/j.mib.2008.10.007>, 2008.
- 795 Franze, T., Weller, M. G., Niessner, R. and Pöschl, U.: Protein nitration by polluted air, *Environ. Sci. Technol.*, 39, 1673–1678, <https://doi.org/10.1021/es0488737>, 2005.



- Fröhlich-Nowoisky, J., Kampf, C. J., Weber, B., Huffman, J. A., Pöhlker, C., Andreae, M. O., Lang-Yona, N., Burrows, S. M., Gunthe, S. S., Elbert, W., Su, H., Hoor, P., Thines, E., Hoffmann, T., Després, V. R. and Pöschl, U.: Bioaerosols in the Earth system: Climate, health, and ecosystem interactions, *Atmos. Res.*, 800 182, 346–376, <https://doi.org/10.1016/j.atmosres.2016.07.018>, 2016.
- Gérard, V., Noziere, B., Fine, L., Ferronato, C., Singh, D. K., Frossard, A. A., Cohen, R. C., Asmi, E., Lihavainen, H., Kivekäs, N., Aurela, M., Brus, D., Frka, S. and Cvitešić Kušan, A.: Concentrations and Adsorption Isotherms for Amphiphilic Surfactants in PM1 Aerosols from Different Regions of Europe, *Environ. Sci. Technol.*, 53, 12379–12388, <https://doi.org/10.1021/acs.est.9b03386>, 2019.
- 805 Graham, B., Guyon, P., Maenhaut, W., Taylor, P. E., Ebert, M., Matthias-Maser, S., Mayol-Bracero, O. L., Godoi, R. H. M., Artaxo, P., Meixner, F. X., Lima Moura, M. A., Eça D’Almeida Rocha, C. H., Van Grieken, R., Glovsky, M. M., Flagan, R. C. and Andreae, M. O.: Composition and diurnal variability of the natural Amazonian aerosol, *J. Geophys. Res. D Atmos.*, 108, D24, <https://doi.org/10.1029/2003jd004049>, 2003.
- Gunthe, S. S., Rose, D., Su, H., Garland, R. M., Achtert, P., Nowak, A., Wiedensohler, A., Kuwata, M., 810 Takegawa, N., Kondo, Y., Hu, M., Shao, M., Zhu, T., Andreae, M. O. and Pöschl, U.: Cloud condensation nuclei (CCN) from fresh and aged air pollution in the megacity region of Beijing, *Atmos. Chem. Phys.*, 11, 11023–11039, <https://doi.org/10.5194/acp-11-11023-2011>, 2011.
- Gute, E. and Abbatt, J. P. D.: Oxidative Processing Lowers the Ice Nucleation Activity of Birch and Alder Pollen, *Geophys. Res. Lett.*, 45, 1647–1653, <https://doi.org/10.1002/2017GL076357>, 2018.
- 815 Haddrell, A. E. and Thomas, R. J.: Aerobiology: Experimental considerations, observations, and future tools, *Appl. Environ. Microbiol.*, 83, e00809-17, <https://doi.org/10.1128/AEM.00809-17>, 2017.
- Hamilton, W. D. and Lenton, T. M.: Spora and gaia: How microbes fly with their clouds, *Ethol. Ecol. Evol.*, 10, 1–16, <https://doi.org/10.1080/08927014.1998.9522867>, 1998.
- Heald, C. L. and Spracklen, D. V.: Atmospheric budget of primary biological aerosol particles from fungal 820 spores, *Geophys. Res. Lett.*, 36, L09806, <https://doi.org/10.1029/2009GL037493>, 2009.
- Hernandez, M. N. and Lindow, S. E.: *Pseudomonas syringae* increases water availability in leaf microenvironments via production of hygroscopic syringafactin, *Appl. Environ. Microbiol.*, 85, e01014-19, <https://doi.org/10.1128/AEM.01014-19>, 2019.
- Hill, S. C., Williamson, C. C., Doughty, D. C., Pan, Y. Le, Santarpia, J. L. and Hill, H. H.: Size-dependent 825 fluorescence of bioaerosols: Mathematical model using fluorescing and absorbing molecules in bacteria, *J. Quant. Spectrosc. Radiat. Transf.*, 157, 54–70, <https://doi.org/10.1016/j.jqsrt.2015.01.011>, 2015.
- Hoose, C. and Möhler, O.: Heterogeneous ice nucleation on atmospheric aerosols: A review of results from



- laboratory experiments., *Atmos. Chem. Phys.*, 12, 9817–9854, <https://doi.org/10.5194/acp-12-9817-2012>, 2012
- 830 Hoose, C., Kristjánsson, J. E. and Burrows, S. M.: How important is biological ice nucleation in clouds on a global scale?, *Environ. Res. Lett.*, 5, 024009, <https://doi.org/10.1088/1748-9326/5/2/024009>, 2010.
- Horneck, G., Bücker, H. and Reitz, G.: Long-term survival of bacterial spores in space, *Adv. Sp. Res.*, 14, 41–45, [https://doi.org/10.1016/0273-1177\(94\)90448-0](https://doi.org/10.1016/0273-1177(94)90448-0), 1994.
- Hu, W., Niu, H., Murata, K., Wu, Z., Hu, M., Kojima, T. and Zhang, D.: Bacteria in atmospheric waters:
835 Detection, characteristics and implications, *Atmos. Environ.*, 179, 201–221, <https://doi.org/10.1016/j.atmosenv.2018.02.026>, 2018.
- Hu, Y., Zhao, X., Gu, Y., Chen, X., Wang, X., Wang, P., Zheng, Z. and Dong, X.: Significant broadband extinction abilities of bioaerosols, *Sci. China Mater.*, 62, 1033–1045, <https://doi.org/10.1007/s40843-018-9411-9>, 2019.
- 840 Huffman, J. A., Treutlein, B. and Pöschl, U.: Fluorescent biological aerosol particle concentrations and size distributions measured with an Ultraviolet Aerodynamic Particle Sizer (UV-APS) in Central Europe, *Atmos. Chem. Phys.*, 10, 3215–3233, <https://doi.org/10.5194/acp-10-3215-2010>, 2010.
- Huffman, J. A., Prenni, A. J., Demott, P. J., Pöhlker, C., Mason, R. H., Robinson, N. H., Fröhlich-Nowoisky, J., Tobo, Y., Després, V. R., Garcia, E., Gochis, D. J., Harris, E., Müller-Germann, I., Ruzene, C., Schmer,
845 B., Sinha, B., Day, D. A., Andreae, M. O., Jimenez, J. L., Gallagher, M., Kreidenweis, S. M., Bertram, A. K. and Pöschl, U.: High concentrations of biological aerosol particles and ice nuclei during and after rain, *Atmos. Chem. Phys.*, 13, 6151–6164, <https://doi.org/10.5194/acp-13-6151-2013>, 2013.
- Huffman, J. A., Perring, A. E., Savage, N. J., Clot, B., Crouzy, B., Tummon, F., Shoshanim, O., Damit, B., Schneider, J., Sivaprakasam, V., Zawadowicz, M. A., Crawford, I., Gallagher, M., Topping, D., Doughty,
850 D. C., Hill, S. C. and Pan, Y.: Real-time sensing of bioaerosols: Review and current perspectives, *Aerosol Sci. Technol.*, 54, 465–495, <https://doi.org/10.1080/02786826.2019.1664724>, 2020.
- Jaenicke, R.: Abundance of cellular material and proteins in the atmosphere, *Science*, 308, 73–73, <https://doi.org/10.1126/science.1106335>, 2005.
- Jayaraman, S., Gantz, D. L. and Gursky, O.: Effects of protein oxidation on the structure and stability of
855 model discoidal high-density lipoproteins, *Biochemistry*, 47, 3875–3882, <https://doi.org/10.1021/bi7023783>, 2008.
- Jiaxian, P., Shumin, Z., Kai, X., Junyang, Z., Chuanhe, Y., Senlin, L., Wei, Z., Yuzhen, F., Yuxiang, Y., Xinhui, B., Guohua, Z. and Qingyue, W.: Diversity of bacteria in cloud water collected at a National



860 Atmospheric Monitoring Station in Southern China, *Atmos. Res.*, 218, 176-182,
<https://doi.org/10.1016/j.atmosres.2018.12.004>, 2019.

Joly, M., Attard, E., Sancelme, M., Deguillaume, L., Guilbaud, C., Morris, C. E., Amato, P. and Delort, A. M.: Ice nucleation activity of bacteria isolated from cloud water, *Atmos. Environ.*, 70, 392-400,
<https://doi.org/10.1016/j.atmosenv.2013.01.027>, 2013.

865 Joly, M., Amato, P., Sancelme, M., Vinatier, V., Abrantes, M., Deguillaume, L. and Delort, A. M.: Survival
of microbial isolates from clouds toward simulated atmospheric stress factors, *Atmos. Environ.*, 117, 92-98,
<https://doi.org/10.1016/j.atmosenv.2015.07.009>, 2015.

Junge, K. and Swanson, B. D.: High-resolution ice nucleation spectra of sea-ice bacteria: Implications for
cloud formation and life in frozen environments, *Biogeosciences*, 5, 865–873, <https://doi.org/10.5194/bg-5-865-2008>, 2008.

870 Kang, H., Xie, Z. and Hu, Q.: Ambient protein concentration in PM10 in Hefei, central China, *Atmos.
Environ.*, 54, 73-79, <https://doi.org/10.1016/j.atmosenv.2012.03.003>, 2012.

Khaled, A., M. Zhang, P. Amato, A. Delort, and B. Ervens, Biodegradation by bacteria in clouds: An
underestimated sink for some organics in the atmospheric multiphase system, *Atmos. Chem. Phys.*,
submitted, 2020.

875 Kjelleberg, S. and Hermansson, M.: Starvation-induced effects on bacterial surface characteristics, *Appl.
Environ. Microbiol.*, 48, 497-503, <https://doi.org/10.1128/aem.48.3.497-503.1984>, 1984.

Konstantinidis, K. T.: Do airborne microbes matter for atmospheric chemistry and cloud formation?,
Environ. Microbiol., 16, 1482-1484, <https://doi.org/10.1111/1462-2920.12396>, 2014.

880 Kristinsson, H. G. and Hultin, H. O.: Changes in trout hemoglobin conformations and solubility after
exposure to acid and alkali pH, *J. Agric. Food Chem.*, 52, 3633-3643, <https://doi.org/10.1021/jf034563g>, 2004.

Kunert, A. T., Pöhlker, M. L., Tang, K., Krevert, C. S., Wieder, C., Speth, K. R., Hanson, L. E., Morris, C.
E., Schmale, D. G., Pöschl, U. and Fröhlich-Nowoisky, J.: Macromolecular fungal ice nuclei in *Fusarium*:
Effects of physical and chemical processing, *Biogeosciences*, 16, 4647–4659, <https://doi.org/10.5194/bg-16-4647-2019>, 2019.

885 Lee, B. U., Kim, S. H. and Kim, S. S.: Hygroscopic growth of *E. Coli* and *B. Subtilis* bioaerosols, *J. Aerosol
Sci.*, 33, 1721-1723, [https://doi.org/10.1016/S0021-8502\(02\)00114-3](https://doi.org/10.1016/S0021-8502(02)00114-3), 2002.

Lelieveld, J. and Crutzen, P. J.: Influences of cloud photochemical processes on tropospheric ozone, *Nature*,
343, 227-233, <https://doi.org/10.1038/343227a0>, 1990.



- Lighthart, B.: The ecology of bacteria in the al fresco atmosphere, *FEMS Microbiol. Ecol.*, 23, 263-274,
890 [https://doi:10.1016/S0168-6496\(97\)00036-6](https://doi:10.1016/S0168-6496(97)00036-6), 1997.
- Lighthart, B. and Shaffer, B. T.: Viable bacterial aerosol particle size distributions in the midsummer atmosphere at an isolated location in the high desert chaparral, *Aerobiologia*, 11,19-25,
<https://doi:10.1007/BF02136140>, 1995.
- Liu, C. and Yin, Y.: Inherent optical properties of pollen particles: a case study for the morning glory pollen,
895 *Opt. Express*, 24, A104-A113, <https://doi:10.1364/oe.24.00a104>, 2016.
- Liu, P. F., Abdelmalki, N., Hung, H. M., Wang, Y., Brune, W. H. and Martin, S. T.: Ultraviolet and visible complex refractive indices of secondary organic material produced by photooxidation of the aromatic compounds toluene and m-xylene, *Atmos. Chem. Phys.*, 15, 1435–1446, <https://doi:10.5194/acp-15-1435-2015>, 2015.
- 900 Löndahl, J., Möller, W., Pagels, J. H., Kreyling, W. G., Swietlicki, E. and Schmid, O.: Measurement techniques for respiratory tract deposition of airborne nanoparticles: A critical review, *J. Aerosol Med. Pulm. Drug Deliv.*, 27, 229-254, <https://doi:10.1089/jamp.2013.1044>, 2014.
- Lowe, S. J., Partridge, D. G., Davies, J. F., Wilson, K. R., Topping, D. and Riipinen, I.: Key drivers of cloud response to surface-active organics, *Nat. Commun.*, 10, 1-12, <https://doi:10.1038/s41467-019-12982-0>,
905 2019.
- Lukas, M., Schwidetzky, R., Kunert, A. T., Pöschl, U., Fröhlich-Nowoisky, J., Bonn, M. and Meister, K.: Electrostatic Interactions Control the Functionality of Bacterial Ice Nucleators, *J. Am. Chem. Soc.*, 142, 6842-6846, <https://doi:10.1021/jacs.9b13069>, 2020.
- Marr, A. G.: Growth rate of *Escherichia coli*, *Microbiol. Rev.*, 55, 316-333,
910 <https://doi:10.1128/mmbr.55.2.316-333.1991>, 1991.
- Matthias-Maser, S., Brinkmann, J. and Schneider, W.: The size distribution of marine atmospheric aerosol with regard to primary biological aerosol particles over the South Atlantic Ocean, *Atmos. Environ.*, 33, 3569-3575, [https://doi:10.1016/S1352-2310\(98\)00121-6](https://doi:10.1016/S1352-2310(98)00121-6), 1999.
- Matthias-Maser, S., Obolkin, V., Khodzer, T. and Jaenicke, R.: Seasonal variation of primary biological
915 aerosol particles in the remote continental region of Lake Baikal/Siberia, *Atmos. Environ.*, 34, 3805-3811, [https://doi:10.1016/S1352-2310\(00\)00139-4](https://doi:10.1016/S1352-2310(00)00139-4), 2000a.
- Matthias-Maser, S., Bogs, B. and Jaenicke, R.: The size distribution of primary biological aerosol particles in cloud water on the mountain Kleiner Feldberg/Taunus (FRG), *Atmos. Res.*, 54, 1-13, [https://doi:10.1016/S0169-8095\(00\)00039-9](https://doi:10.1016/S0169-8095(00)00039-9), 2000b.



- 920 Middelboe, M.: Bacterial growth rate and marine virus-host dynamics, *Microb. Ecol.*, 40, 114-124, <https://doi.org/10.1007/s002480000050>, 2000.
- Moise, T., Flores, J. M. and Rudich, Y.: Optical Properties of Secondary Organic Aerosols and Their Changes by Chemical Processes, *Chem. Rev.*, 115, 4400–4439, <https://doi.org/10.1021/cr5005259>, 2015.
- Monier, J. M. and Lindow, S. E.: Differential survival of solitary and aggregated bacterial cells promotes
925 aggregate formation on leaf surfaces, *Proc. Natl. Acad. Sci. U. S. A.*, 100, 15977-15982, <https://doi.org/10.1073/pnas.2436560100>, 2003.
- Monier, J. M. and Lindow, S. E.: Aggregates of resident bacteria facilitate survival of immigrant bacteria on leaf surfaces, *Microb. Ecol.*, 49, 343-352, <https://doi.org/10.1007/s00248-004-0007-9>, 2005.
- Morris, C. E., Georgakopoulos, D. G. and Sands, D. C.: Ice nucleation active bacteria and their potential
930 role in precipitation, *J. Phys. IV France*, 121, 87-103, <https://doi.org/10.1051/jp4:2004121004>, 2004.
- Morris, C. E., Sands, D. C., Vinatzer, B. A., Glaux, C., Guilbaud, C., Buffière, A., Yan, S., Dominguez, H. and Thompson, B. M.: The life history of the plant pathogen *Pseudomonas syringae* is linked to the water cycle, *ISME J.*, 2, 321-334, <https://doi.org/10.1038/ismej.2007.113>, 2008.
- Neu, T. R.: Significance of bacterial surface-active compounds in interaction of bacteria with interfaces,
935 *Microbiol. Rev.*, 60, 151, <https://doi.org/10.1128/membr.60.1.151-166.1996>, 1996.
- Nozière, B., Baduel, C. and Jaffrezo, J. L.: The dynamic surface tension of atmospheric aerosol surfactants reveals new aspects of cloud activation, *Nat. Commun.*, 5, 1-7, <https://doi.org/10.1038/ncomms4335>, 2014.
- Ovadnevaite, J., Zuend, A., Laaksonen, A., Sanchez, K. J., Roberts, G., Ceburnis, D., Decesari, S., Rinaldi, M., Hodas, N., Facchini, M. C., Seinfeld, J. H. and O'Dowd, C.: Surface tension prevails over solute effect
940 in organic-influenced cloud droplet activation, *Nature*, 546, 637-641, <https://doi.org/10.1038/nature22806>, 2017.
- Petters, M. D. and Kreidenweis, S. M.: A single parameter representation of hygroscopic growth and cloud condensation nucleus activity, *Atmos. Chem. Phys.*, 7, 1961–1971, <https://doi.org/10.5194/acp-7-1961-2007>, 2007.
- 945 Pope, F. D.: Pollen grains are efficient cloud condensation nuclei, *Environ. Res. Lett.*, 5, 044015, <https://doi.org/10.1088/1748-9326/5/4/044015>, 2010.
- Pöschl, U.: Atmospheric aerosols: Composition, transformation, climate and health effects, *Angew. Chemie - Int. Ed.*, 44, 7520-7540, <https://doi.org/10.1002/anie.200501122>, 2005.
- Pöschl, U. and Shiraiwa, M.: Multiphase Chemistry at the Atmosphere-Biosphere Interface Influencing



- 950 Climate and Public Health in the Anthropocene, *Chem. Rev.*, 115, 4440-4475,
<https://doi.org/10.1021/cr500487s>, 2015.
- Pósfai, M., Xu, H., Anderson, J. R. and Buseck, P. R.: Wet and dry sizes of atmospheric aerosol particles:
An AFM-TEM Study, *Geophys. Res. Lett.*, 25, 1907–1910, <https://doi.org/10.1029/98gl01416>, 1998.
- Pouzet, G., Peghaire, E., Aguès, M., Baray, J. L., Conen, F. and Amato, P.: Atmospheric processing and
955 variability of biological ice nucleating particles in precipitation at Opme, France, *Atmosphere*, 8, 229,
<https://doi.org/10.3390/atmos8110229>, 2017.
- Pratt, K. A., Demott, P. J., French, J. R., Wang, Z., Westphal, D. L., Heymsfield, A. J., Twohy, C. H., Prenni,
A. J. and Prather, K. A.: In situ detection of biological particles in cloud ice-crystals, *Nat. Geosci.*, 2, 398–
401, <https://doi.org/10.1038/ngeo521>, 2009.
- 960 Prenni, A. J., Petters, M. D., Kreidenweis, S. M., Heald, C. L., Martin, S. T., Artaxo, P., Garland, R. M.,
Wollny, A. G. and Pöschl, U.: Relative roles of biogenic emissions and saharan dust as ice nuclei in the
amazon basin, *Nat. Geosci.*, 2, 402–405, <https://doi.org/10.1038/ngeo517>, 2009.
- Price, P. B. and Sowers, T.: Temperature dependence of metabolic rates for microbial growth, maintenance,
and survival, *Proc. Natl. Acad. Sci. U. S. A.*, 101, 4631-4636, <https://doi.org/10.1073/pnas.0400522101>, 2004.
- 965 Prisle, N. L., Lin, J. J., Purdue, S., Lin, H., Carson Meredith, J. and Nenes, A.: Cloud condensation nuclei
activity of six pollenkits and the influence of their surface activity, *Atmos. Chem. Phys.*, 19, 4741–4761,
<https://doi.org/10.5194/acp-19-4741-2019>, 2019.
- Pruppacher, H. R. and Klett, J. D.: *Microphysics of clouds and precipitation*, Kluwer Academic Publishers,
Dordrecht, the Netherlands, 1997.
- 970 Prussin, A. J., Garcia, E. B. and Marr, L. C.: Total concentrations of virus and bacteria in indoor and outdoor
air, *Environ. Sci. Technol. Lett.*, 2, 84-88, <https://doi.org/10.1021/acs.estlett.5b00050>, 2015.
- Pšenčík, J., Ikonen, T. P., Laurinmäki, P., Merckel, M. C., Butcher, S. J., Serimaa, R. E. and Tuma, R.:
Lamellar organization of pigments in chlorosomes, the light harvesting complexes of green photosynthetic
bacteria, *Biophys. J.*, 87, 1165-1172, <https://doi.org/10.1529/biophysj.104.040956>, 2004.
- 975 Renard, P., Canet, I., Sancelme, M., Wirgot, N., Deguillaume, L. and Delort, A. M.: Screening of cloud
microorganisms isolated at the Puy de Dôme (France) station for the production of biosurfactants, *Atmos.*
Chem. Phys., 16, 12347–12358, <https://doi.org/10.5194/acp-16-12347-2016>, 2016.
- Rose, D., Gunthe, S. S., Mikhailov, E., Frank, G. P., Dusek, U., Andreae, M. O. and Pöschl, U.: Calibration
and measurement uncertainties of a continuous-flow cloud condensation nuclei counter (DMT-CCNC):
980 CCN activation of ammonium sulfate and sodium chloride aerosol particles in theory and experiment,



- Atmos. Chem. Phys., 8, 1153–1179, <https://doi.org/10.5194/acp-8-1153-2008>, 2008.
- Ruehl, C. R., Davies, J. F. and Wilson, K. R.: An interfacial mechanism for cloud droplet formation on organic aerosols, *Science*, 351, 1447-1450, <https://doi.org/10.1126/science.aad4889>, 2016.
- 985 Sahyoun, M., Korsholm, U. S., Sørensen, J. H., Šantl-Temkiv, T., Finster, K., Gosewinkel, U. and Nielsen, N. W.: Impact of bacterial ice nucleating particles on weather predicted by a numerical weather prediction model, *Atmos. Environ.*, 170, 33-44, <https://doi.org/10.1016/j.atmosenv.2017.09.029>, 2017.
- Šantl-Temkiv, T., Sikoparija, B., Maki, T., Carotenuto, F., Amato, P., Yao, M., Morris, C. E., Schnell, R., Jaenicke, R., Pöhlker, C., DeMott, P. J., Hill, T. C. J. and Huffman, J. A.: Bioaerosol field measurements: Challenges and perspectives in outdoor studies, *Aerosol Sci. Technol.*, 54, 520-546,
990 <https://doi.org/10.1080/02786826.2019.1676395>, 2020.
- Sattler, B., Puxbaum, H. and Psenner, R.: Bacterial growth in supercooled cloud droplets, *Geophys. Res. Lett.*, 28, 239-242, <https://doi.org/10.1029/2000GL011684>, 2001.
- Schneider, J., Freutel, F., Zorn, S. R., Chen, Q., Farmer, D. K., Jimenez, J. L., Martin, S. T., Artaxo, P., Wiedensohler, A. and Borrmann, S.: Mass-spectrometric identification of primary biological particle
995 markers and application to pristine submicron aerosol measurements in Amazonia, *Atmos. Chem. Phys.*, 11, 11415–11429, <https://doi.org/10.5194/acp-11-11415-2011>, 2011.
- Schumacher, C. J., Pöhlker, C., Aalto, P., Hiltunen, V., Petäjä, T., Kulmala, M., Pöschl, U. and Huffman, J. A.: Seasonal cycles of fluorescent biological aerosol particles in boreal and semi-arid forests of Finland and Colorado, *Atmos. Chem. Phys.*, 13, 11987–12001, <https://doi.org/10.5194/acp-13-11987-2013>, 2013.
- 1000 Sesartic, A., Lohmann, U. and Storelvmo, T.: Bacteria in the ECHAM5-HAM global climate model, *Atmos. Chem. Phys.*, 12, 8645–8661, <https://doi.org/10.5194/acp-12-8645-2012>, 2012.
- Setlow, P.: I will survive: DNA protection in bacterial spores, *Trends Microbiol.*, 15, 172-180, <https://doi.org/10.1016/j.tim.2007.02.004>, 2007.
- Shen, F., Zheng, Y., Niu, M., Zhou, F., Wu, Y., Wang, J., Zhu, T., Wu, Y., Wu, Z., Hu, M. and Zhu, T.:
1005 Characteristics of biological particulate matters at urban and rural sites in the North China Plain, *Environ. Pollut.*, 253, 569-577, <https://doi.org/10.1016/j.envpol.2019.07.033>, 2019.
- Sheng, G. P., Yu, H. Q. and Li, X. Y.: Extracellular polymeric substances (EPS) of microbial aggregates in biological wastewater treatment systems: A review, *Biotechnol. Adv.*, 28, 882-894, <https://doi.org/10.1016/j.biotechadv.2010.08.001>, 2010.
- 1010 Shiraiwa, M., Selzle, K., Yang, H., Sosedova, Y., Ammann, M. and Pöschl, U.: Multiphase chemical kinetics of the nitration of aerosolized protein by ozone and nitrogen dioxide, *Environ. Sci. Technol.*, 46, 6672-6680,



- <https://doi.org/10.1021/es300871b>, 2012.
- Smets, W., Moretti, S., Denys, S. and Lebeer, S.: Airborne bacteria in the atmosphere: Presence, purpose, and potential, *Atmos. Environ.*, 139, 214-221, <https://doi.org/10.1016/j.atmosenv.2016.05.038>, 2016.
- 1015 Stevens, B. and Feingold, G.: Untangling aerosol effects on clouds and precipitation in a buffered system, *Nature*, 461, 607-613, <https://doi.org/10.1038/nature08281>, 2009.
- Stocker, T. F., Dahe, Q., and Plattner, G.-K.: *Climate Change 2013: The Physical Science Basis*, Working Group I Contribution to the Fifth Assessment Report of the Intergovernmental Panel on Climate Change, Summary for Policymakers (IPCC, 2013), 2013.
- 1020 Sun, J. and Ariya, P. A.: Atmospheric organic and bio-aerosols as cloud condensation nuclei (CCN): A review, *Atmos. Environ.*, 40, 795-820, <https://doi.org/10.1016/j.atmosenv.2005.05.052>, 2006.
- Tang, M., Gu, W., Ma, Q., Jie Li, Y., Zhong, C., Li, S., Yin, X., Huang, R. J., He, H. and Wang, X.: Water adsorption and hygroscopic growth of six anemophilous pollen species: The effect of temperature, *Atmos. Chem. Phys.*, 19, 2247–2258, <https://doi.org/10.5194/acp-19-2247-2019>, 2019.
- 1025 Thrush, E., Brown, D. M., Salciccioli, N., Gomes, J., Brown, A., Siegrist, K., Thomas, M. E., Boggs, N. T. and Carter, C. C.: Optical properties and cross-sections of biological aerosols, *Proc. SPIE* 7665, <https://doi.org/10.1117/12.850464>, 2010.
- Tobo, Y., Prenni, A. J., Demott, P. J., Huffman, J. A., McCluskey, C. S., Tian, G., Pöhlker, C., Pöschl, U. and Kreidenweis, S. M.: Biological aerosol particles as a key determinant of ice nuclei populations in a forest ecosystem, *J. Geophys. Res. Atmos.*, 118, 10100-10110, <https://doi.org/10.1002/jgrd.50801>, 2013.
- 1030 Tolocka, M. P., Jang, M., Ginter, J. M., Cox, F. J., Kamens, R. M. and Johnston, M. V.: Formation of Oligomers in Secondary Organic Aerosol, *Environ. Sci. Technol.*, 38, 1428-1434, <https://doi.org/10.1021/es035030r>, 2004.
- Tong, Y. and Lighthart, B.: The annual bacterial particle concentration and size distribution in the ambient atmosphere in a rural area of the Willamette Valley, Oregon, *Aerosol Sci. Technol.*, 32, 393-403, <https://doi.org/10.1080/027868200303533>, 2000.
- 1035 Vařtilingom, M., Amato, P., Sancelme, M., Laj, P., Leriche, M. and Delort, A. M.: Contribution of microbial activity to carbon chemistry in clouds, *Appl. Environ. Microbiol.*, 76, 23-29, <https://doi.org/10.1128/AEM.01127-09>, 2010.
- 1040 Valsan, A. E., Priyamvada, H., Ravikrishna, R., Després, V. R., Biju, C. V., Sahu, L. K., Kumar, A., Verma, R. S., Philip, L. and Gunthe, S. S.: Morphological characteristics of bioaerosols from contrasting locations in southern tropical India - A case study, *Atmos. Environ.*, 122, 321-331,



- https://doi:10.1016/j.atmosenv.2015.09.071, 2015.
- Verreault, D., Moineau, S. and Duchaine, C.: Methods for Sampling of Airborne Viruses, *Microbiol. Mol. Biol. Rev.*, 72, 413-444, <https://doi:10.1128/membr.00002-08>, 2008.
- 1045
- Vrede, K., Heldal, M., Norland, S. and Bratbak, G.: Elemental composition (C, N, P) and cell volume of exponentially growing and nutrient-limited bacterioplankton, *Appl. Environ. Microbiol.*, 68, 2965-2971, <https://doi:10.1128/AEM.68.6.2965-2971.2002>, 2002.
- Weesendorp, E., Landman, W. J. M., Stegeman, A. and Loeffen, W. L. A.: Detection and quantification of classical swine fever virus in air samples originating from infected pigs and experimentally produced aerosols, *Vet. Microbiol.*, 127, 50-62, <https://doi:10.1016/j.vetmic.2007.08.013>, 2008.
- 1050
- Wei, K., Zou, Z., Zheng, Y., Li, J., Shen, F., Wu, C. yu, Wu, Y., Hu, M. and Yao, M.: Ambient bioaerosol particle dynamics observed during haze and sunny days in Beijing, *Sci. Total Environ.*, 550, 751-759, <https://doi:10.1016/j.scitotenv.2016.01.137>, 2016.
- 1055
- Wittmaack, K., Wehnes, H., Heinzmann, U. and Agerer, R.: An overview on bioaerosols viewed by scanning electron microscopy, *Sci. Total Environ.*, 346, 244-255, <https://doi:10.1016/j.scitotenv.2004.11.009>, 2005.
- Wu, Y., Chen, A., Luhung, I., Gall, E. T., Cao, Q., Chang, V. W. C. and Nazaroff, W. W.: Bioaerosol deposition on an air-conditioning cooling coil, *Atmos. Environ.*, 144, 257-265, <https://doi:10.1016/j.atmosenv.2016.09.004>, 2016.
- 1060
- Xie, B., Gu, J. and Lu, J.: Surface properties of bacteria from activated sludge in relation to bioflocculation, *J. Environ. Sci.*, 22, 1840-1845, [https://doi:10.1016/S1001-0742\(09\)60329-6](https://doi:10.1016/S1001-0742(09)60329-6), 2010.
- Yu, X., Wang, Z., Zhang, M., Kuhn, U., Xie, Z., Cheng, Y., Pöschl, U. and Su, H.: Ambient measurement of fluorescent aerosol particles with a WIBS in the Yangtze River Delta of China: Potential impacts of combustion-related aerosol particles, *Atmos. Chem. Phys.*, 16, 11337-11348, <https://doi:10.5194/acp-16-11337-2016>, 2016.
- 1065
- Zhang, M., Klimach, T., Ma, N., Könemann, T., Pöhlker, C., Wang, Z., Kuhn, U., Scheck, N., Pöschl, U., Su, H. and Cheng, Y.: Size-Resolved Single-Particle Fluorescence Spectrometer for Real-Time Analysis of Bioaerosols: Laboratory Evaluation and Atmospheric Measurements, *Environ. Sci. Technol.*, 53, 13257-13264, <https://doi:10.1021/acs.est.9b01862>, 2019.

1070